CONTAMINATION DETECTION ON AIR BEARING SURFACE

CHIEWCHAN TANGKONGKIET

A THESIS SUBMITTED IN PARTIAL FULFILLMENT

OF THE REQUIREMENT FOR THE DEGREE OF MASTER OF ENGINEERING IN DATA STORAGE TECHNOLOGY

~~FACULTY OF~~ INTERNATIONAL COLLEGE

KING MONGKUT'S INSTITUTE OF TECHNOLOGY LADKRABANG

2013

KMITL-2013-IC-M-005-001

หัวข้อวิทยานิพนธ์	การตรวจสอบการปนเปื้อนบนพื้นผิวแอร์แบริ่ง
นักศึกษา	นายเชี่ยวชาญ ตั้งกองเกียรติ
รหัสประจำตัว	54600704
ปริญญา	วิศวกรรมศาสตรมหาบัณฑิต
สาขาวิชา	เทคโนโลยีการบันทึกข้อมูล
พ.ศ.	2556
อาจารย์ที่ปรึกษาวิทยานิพนธ์	รศ.ดร.ปิติเขต สู้รักษา

บทคัดย่อ

พื้นผิวแอร์แบริ่ง (ABS) เป็นส่วนประกอบที่สำคัญของการอ่านและเขียนของอุปกรณ์บันทึกข้อมูลแบบแข็ง (Hard-Disk Drive, HDD) ปัจจุบันการตรวจสอบการปนเปื้อนจะทำโดยมนุษย์และกล้องจุลทรรศน์ ปัญหาหลักในการตรวจสอบ ABS ด้วยเครื่องจักรแบบวิทัศน์ในกระบวนการผลิตคือความแปรปรวนของความคมชัดของ ABS งานวิจัยนี้เสนอวิธีการใหม่สำหรับการลดการแปรปรวนของความคมชัดของ ABS โดยใช้การเพิ่มประสิทธิของความคมชัดของภาพ (Contrast enhancement) แล้วแยกคุณลักษณะของ ABS โดยใช้การวิเคราะห์องค์ประกอบหลัก (Principal Component Analysis, PCA) และจากนั้นเลือกเกณฑ์สำหรับจัดกลุ่ม ABS ที่มีความบกพร่องและไม่มีความบกพร่องโดยกำหนดเกณฑ์จากผลรวมของข้อผิดพลาดสองชนิดที่น้อยที่สุดคือการอนุญาตผิดพลาดและการปฏิเสธผิดพลาด การทดลองแสดงให้เห็นว่า PCA และการเพิ่มประสิทธิภาพความคมชัดของภาพสามารถแยก ABS ที่มีความบกพร่องและไม่มีความบกพร่องได้อย่างชัดเจน จากผลลัพท์เป็นการยืนยันประโยชน์ของ PCA และการเพิ่มประสิทธิภาพความคมชัดของภาพว่าเป็นเครื่องมือที่มีประสิทธิภาพสำหรับเครื่องจักรแบบวิทัศน์

Thesis	Contamination Detection on Air Bearing Surface
Student	Mr.Chiewchan Tangkongkiet
Student ID.	54600704
Degree	Master of Engineering
Program	Data Storage Technology
Year	2013
Thesis Advisor	Assoc.Prof.Dr. Pitikhate Sooraksa

ABSTRACT

Air Bearing Surface (ABS) is an important feature of a read and writes head in a Hard Disk Drive (HDD). Currently, contamination inspections are carried out by human operators and microscopes. The main problem of inspecting ABS using machine vision in the manufacturing process is contrast variation on the ABS. This research proposes new method for the reduction of contrast variation on the ABS by using Contrast Enhancement, extracting the feature of ABS using Principal Component Analysis (PCA), and selecting the threshold for clustering defected and non-defected ABS. Means of a threshold set has a minimum summation of two types of errors which are false rejection and false acceptance from training data. The experimental results show that PCA with contrast enhancement can clearly separate defect and non-defect ABS. The result confirms its utility as an effective tool for machine vision.

ACKNOWLEDGEMENT

I would like to thank Assoc.Prof.Dr. Pitikhate Sooraksa very much for giving me valuable suggestions, useful advices to overcome all the obstacles in the completion this research.

Finally, I am really grateful to my family and Ms. Pimpa Piboonsak for all love, caring and understanding throughout my life.

Chiewchan Tangkongkiet

TABLE OF CONTENTS

TABLE OF CONTENTS (Continue)

LIST OF FIGURES

LIST OF FIGURES (Continue)

Figures Page

LIST OF TABLES

Tables | Page

CHAPTER 1

INTRODUCTION

1.1 Background

Nowadays, Thailand is the top leading exporter of Hard Disk Drive (HDD) in the world, advocated by the government in various areas. Thus, HDD is the essential electrical products influences on Thailand country export index.

HDD is the primary storage location of computer to record and store data by magnetizing ferromagnetic material on the surface of disk platters directionally. Main components of the hard disk drive are classified by working functions and some of these are listed as follows:

- Read-Write Part
- Data Storage Part
- Movement Control Part
- Microelectronic Interconnect Part

Head Gimbal Assembly (HGA) is a main component of the read-write part which is attached to an actuator arm. It is used to support read and write heads attached at the end of slider to read or write data onto the disk platter. The HGA consists of suspension, gimbal and slider head. The suspension is designed to have low stiffness in the pitch and roll direction and high stiffness in the yaw direction. The suspension and the gimbal have essential spring behavior providing a desired vertical force called 'Gram Load' to push the slider towards the disk surface. While the disk is spinning, the slider lifts and flies with extremely close spacing called 'Flying Height' due to air bearing effect. At the same position, the height between the air bearing surface of slider and the base plate is called the 'z-height'. The flying height depends on accuracy and precision of these significant parameters, Gram Load, Roll Static Attitude (RSA), and Pitch Static Attitude (PSA) which controlled through the HDD assembly process. Changing of flying height can lead to a disk failure in which the slider scrapes across the disk or decreasing the performance and capability of HDD.

The sliders are the carriers built to lift the head micro-inches above the media. Air passing under the air bearing surfaces (ABS) provide the required “lift” and their design has to take into account the weight, velocity, and skew to achieve an uniformed flying height as show in Figure 1.1.

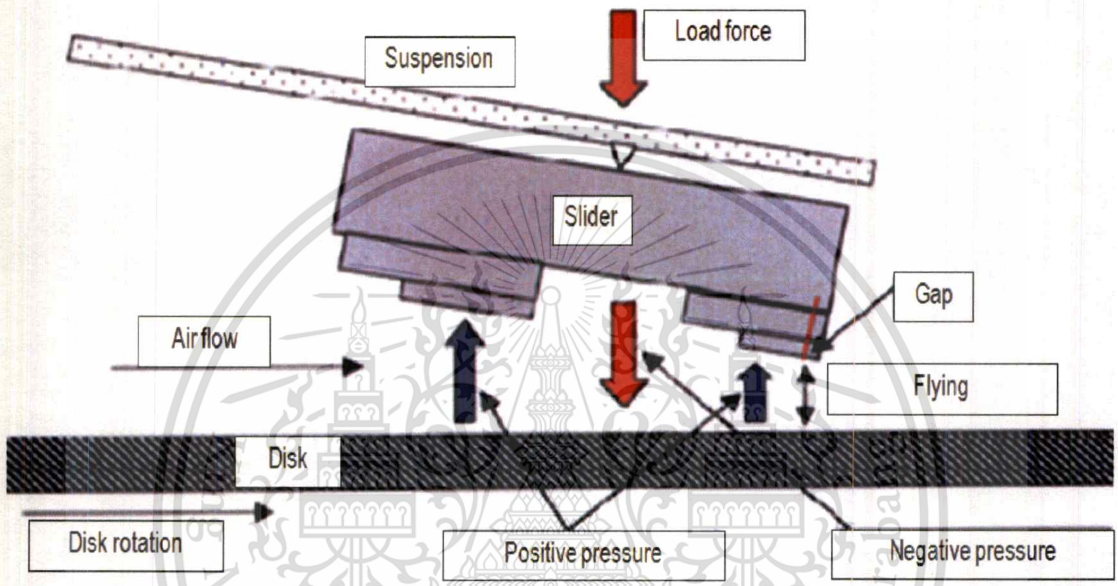

Figure 1.1: Head flying schematic

The flying heights of the sliders have to be very low and flying stability is therefore critical for the air bearing sliders design. Pitch is mainly affected by step recess; roll is affected by side rails or side pads while the trailing pad is correlated to the pitch and flying height. The negative pressure design can improve slider performance with high positive pressure generation and therefore result in high air bearing stiffness at the trailing pad in particular. This allows the slider to follow the waviness of the disk surface better. When the step rail area is increased, there is an increase in pitch with higher positive pressure force at the increased step area. There is also an increase in the flying height due to larger air bearing resultant force. When the area of the trailing edge rail (trailing pad) is increased, the flying height increases and pitch reduces. In track seeking simulation, it is found that the addition of side pads (beside the trailing pad) increases the roll stiffness which stabilizes the slider.

The amplitude of the slider oscillation depends on the air bearing stiffness. The rate of decay of the oscillations depends on the damping ratio of the slider.

The low flying height of the head over the media surface necessities a tight control of the operating environment. Any dust particles, finger prints and other contaminants can cause the head to "crash" on the media surface resulting in damage to the head and media and the possible loss of valuable stored information. Figure 1.2 illustrates the relative dimensions of some possible contaminants compared to the flying height of the disk.

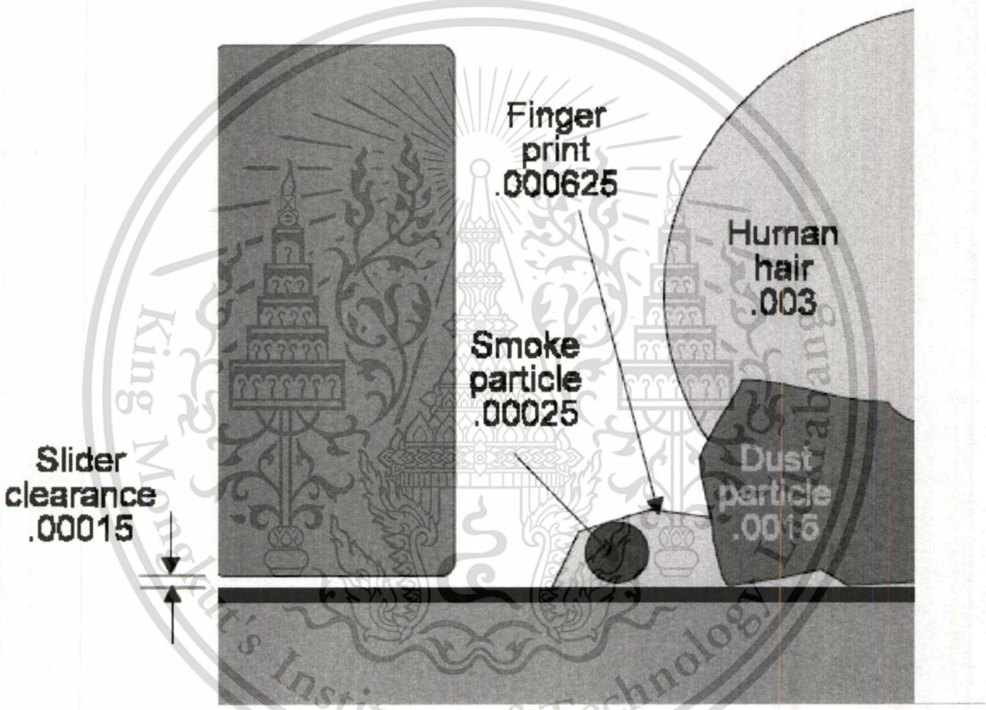

Figure 1.2: Contamination vs. flying

The contamination on air bearing surface could affect on read and write data to be decreased. The lowermost contamination found is the higher efficiency performance of HDD.

Currently, no automatic machine could detect contamination on the air bearing surface. The classification has been done by a human operator detecting under view of microscope. Since the contamination particles are very small, the task is tedious and time consuming due to heavy fatigue loads to human eyes. In addition, the process requires an expert for classification. With this limitation and competence of a human operator working for long hours, this research objective aims to create methodology which could detect the contaminations on the air bearing surface by vision system. The output from this methodology could be reduced unqualified products from the process.

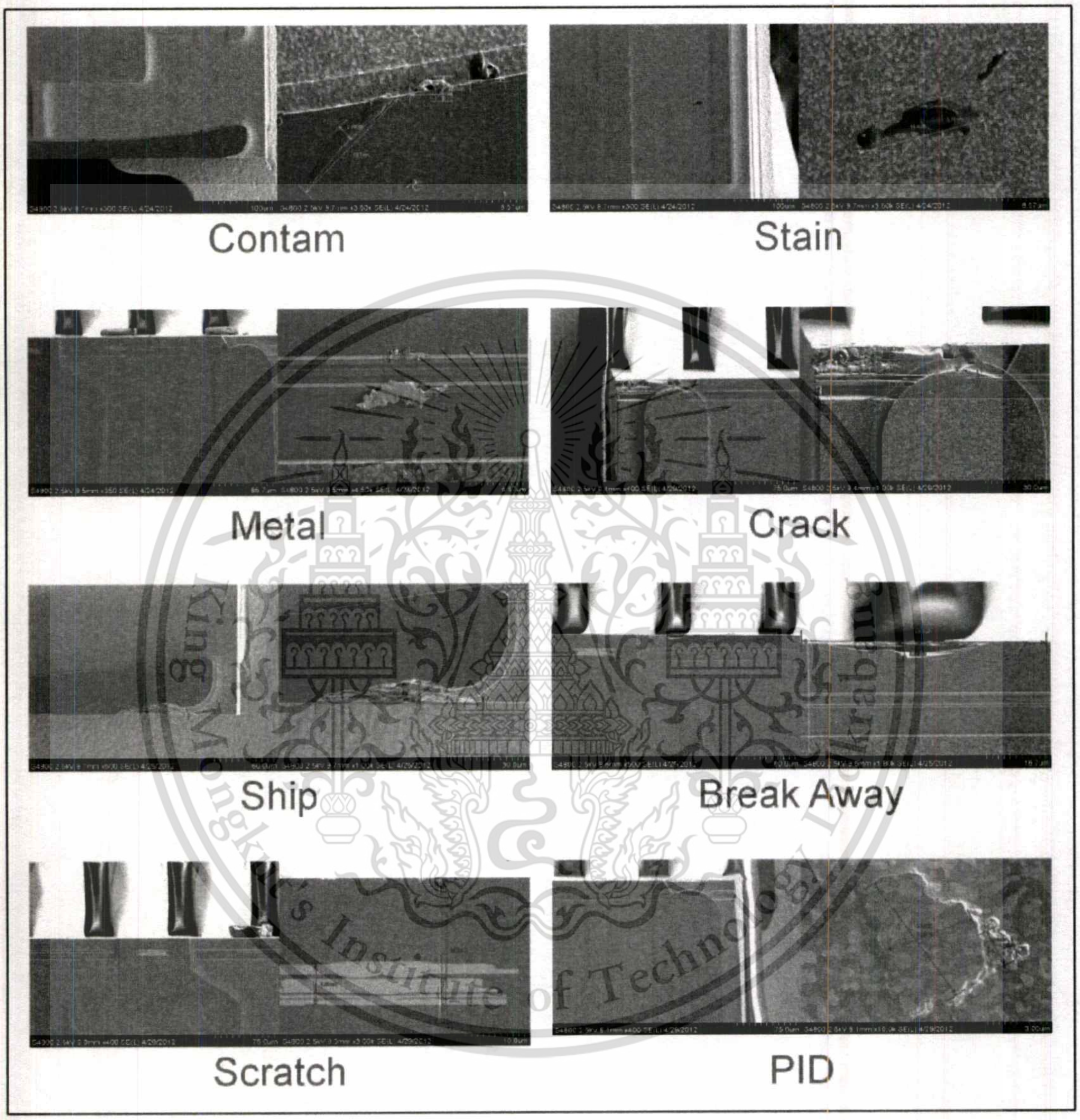

Figure 1.3: Types of contamination from SEM

1.2 Goal

To find out a methodology of a nondestructive test to detect the contamination (only Contam, Stain and Metal type) which is bigger than 5 micrometer on the ABS at the HGA level.

1.3 Scope of work

1. Detecting of the contamination (only Contam, Stain and Metal type) on the ABS at the HGA level is restricted at the laboratory level.
2. In this research, size of the contamination on the air bearing surface is bigger than 5 micrometer.
3. In this research, only 3 types of ABS are studied.

1.4 Benefit

To reduce fatigue of operator' eyes under microscope, after long hour-work, this project causes the quality improvement.

CHAPTER 2

LITERATURE REVIEW

The contamination which might be occurred during HGA process that will cross to ABS could provide lower capability in HDD. There is the studied about the designing, and the impact of contamination, including the characterize which might be contaminated in read/write head and ABS, also Slider as follows;

In 1996, Bo [1] reported results of experimental investigations of contamination build-up on slider surfaces. The conducted investigations into the effects of contamination on the read/write performance include two parts: the reading capability test and the writing capability test. The reading capability test measures the reading performance at different head-disk clearance with the data pre-recorded at a fixed head-disk clearance. The writing capability test was performed by writing the data at different head-disk clearance and reading back the data at a constant head-disk clearance.

For near-contact recording systems, the head-disk clearance variation caused by the contamination can be compared to the designed head-disk clearance and can strongly affect the disk drive's reliability. The variation of head-disk clearance affects the disk drive's performance both in reading and writing operations. The growth in the transition region length in the writing capability test is much greater than the corresponding increase in the head-disk clearance. Measurements of PW50(The width of an isolated readout pulse measured at 50% of its peak amplitude), NLTS and error rate have led to the conclusion that the drive performance, especially the error rate, is quite sensitive to the head-disk clearance variations in the writing process of disk drives with PRML channels. Figure 2.1 - 2.3 show the effects.

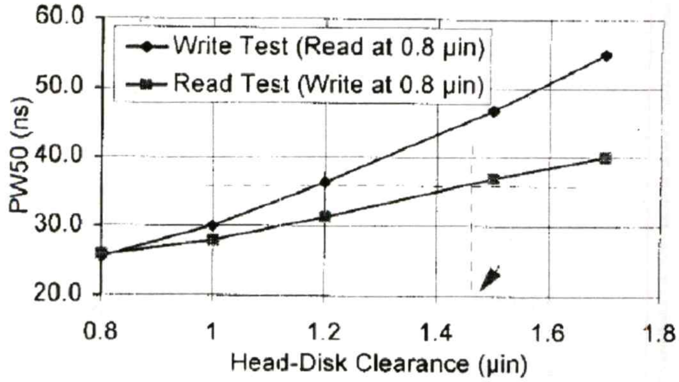

Figure. 2.1: Read/write capability (evaluated by PW50) and head-disk clearance: writing capability is more sensitive to head-disk clearance variation (write current: 8 mA, optimized). [1]

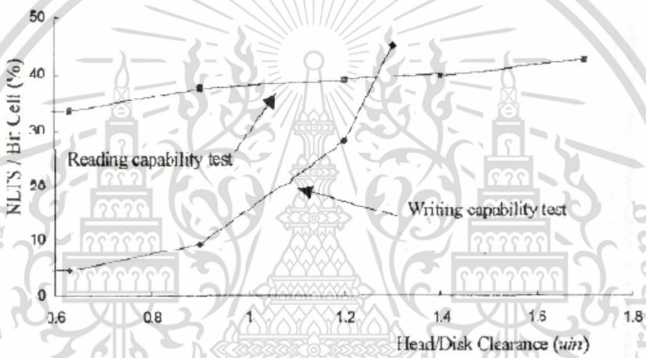

Figure 2.2: NLTS at different head-disk clearance and for both read and write capability test. The NLTS is quite sensitive to head-disk clearance variation in writing process. [1]

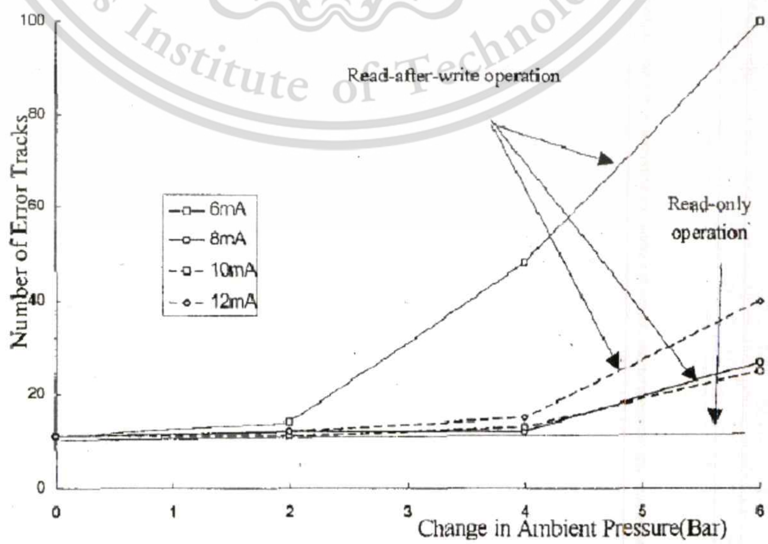

Figure 2.3: Error track number and the increase in head-disk clearance. the head-disk clearance was increased by the increased ambient pressure. [1]

In 1999, Zhang [2] provided mathematical model and the impact of contamination of particles in head and ABS. Through studying the trajectories of the particles, the research team predict several areas on the ABS where the particles are likely to accumulate. These predicted areas are then verified by an experiment designed for testing particle contamination. These methods can be used in slider designs for reducing particle contamination as show in Figures 2.4 - 2.5.

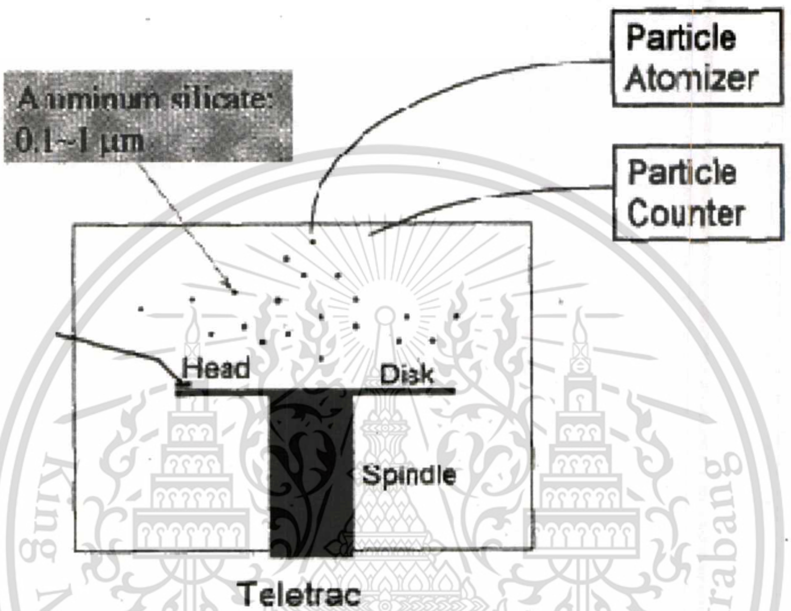

Figure 2.4: Zhang's experimental system. [2]

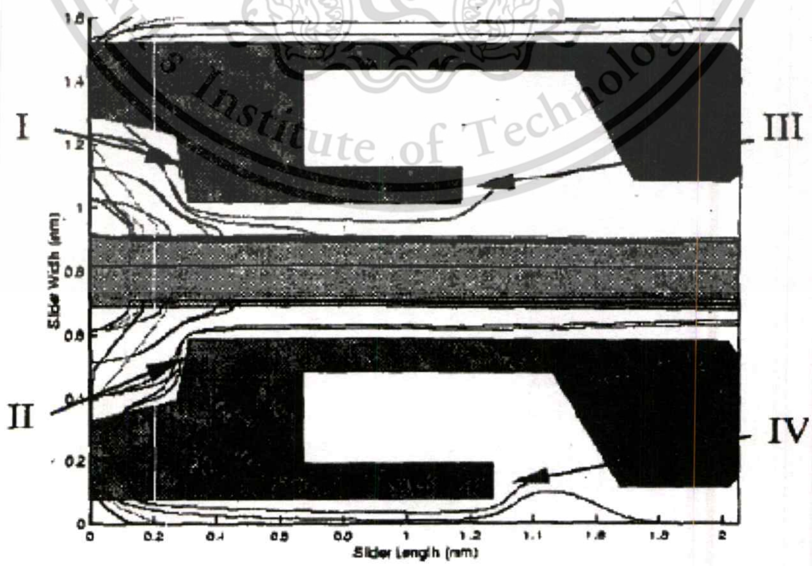

Figure 2.5: X-Y projections of particle paths in the HMI of the modified 7up slider. Shaded areas are ABS and the deep central area. [2]

For the examination with vision system, there were some researchers provided studied in manufacturing industries as follows;

In 1990, He and Wang [3] described a new statistical approach to texture analysis, termed here the texture spectrum approach based on the proposed concept of texture unit. The proposed method extracts the textural information of an image with a more complete respect of texture characteristics. Preliminary evaluations show that the texture spectrum is able to reveal texture information in digital images and that it has promising discriminating performance for different textures. Figures 2.6 - 2.7 show the methodology.

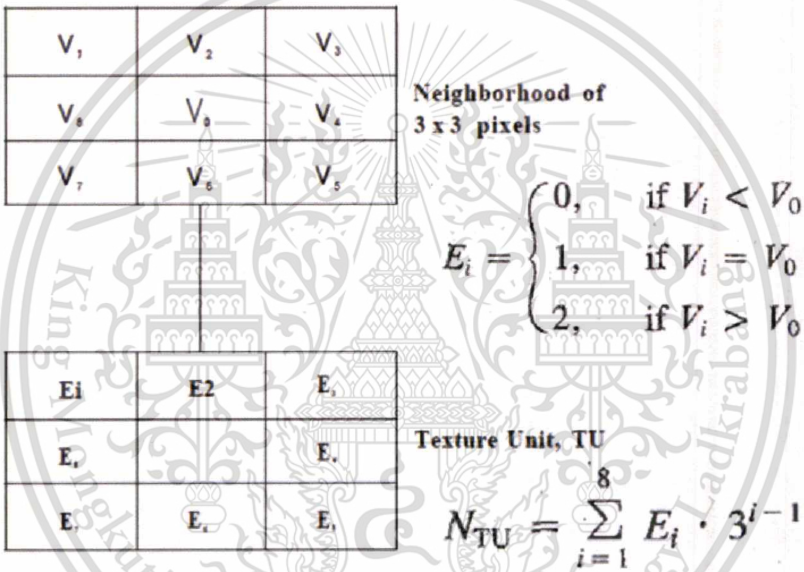

Figure 2.6: Texture unit concept.

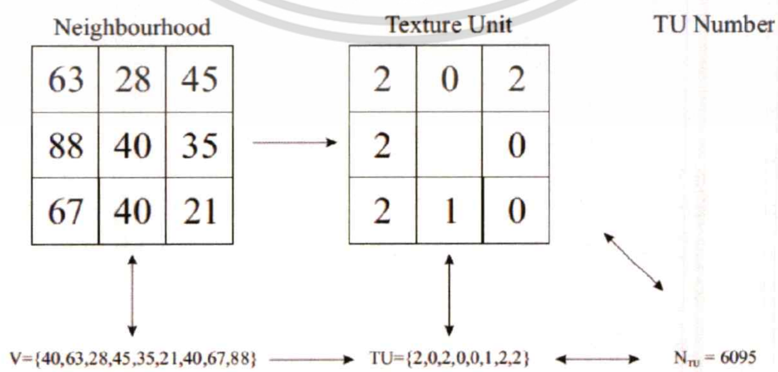

Figure 2.7: Example of transforming a neighborhood to a texture unit with the texture-unit number.

In 1999, Karkanis, Galousi, and Maroulis [4] suggested an approach to texture classification applied on lung endoscopic images. The key concept is to extract all the texture information of an image, by characterizing its textural aspect in the form of a spectrum. They calculate features based on the run lengths of the spectrum image representing the textural descriptors of the respective regions. These measurement are used in a classification based on the stability quotient measured between the different regions. The results given have high accuracy examination. The proposed scheme has been successfully applied on different endoscopic images for the right classification between normal and cancer regions shown in Figure 2.8.

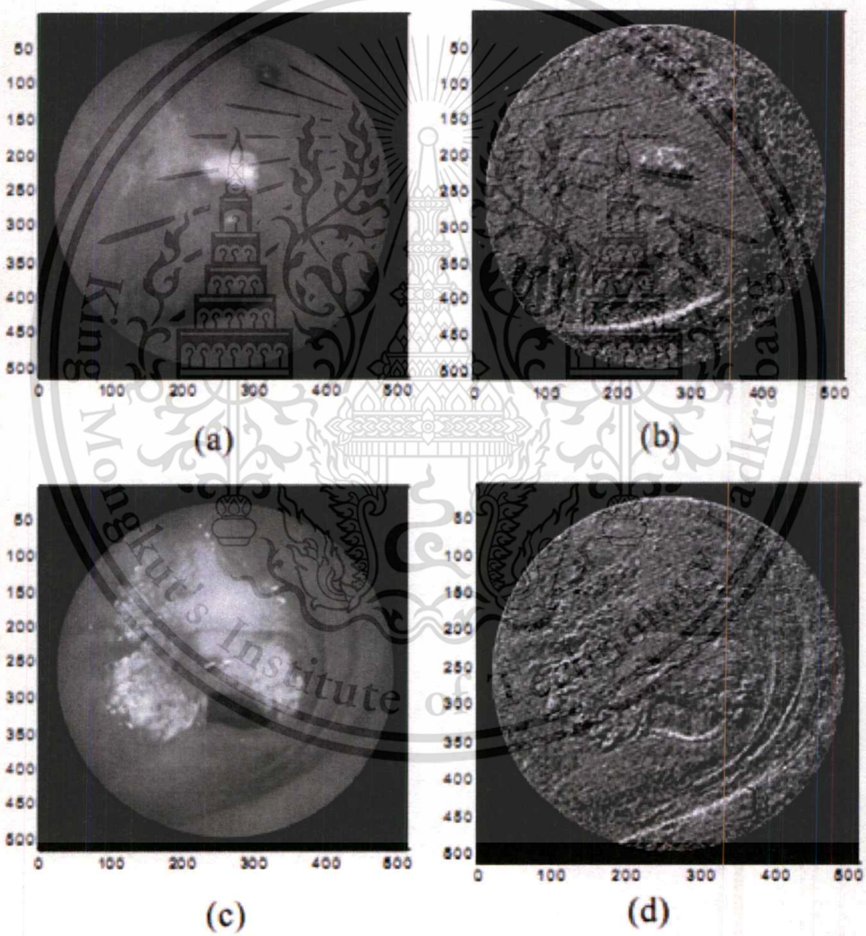

Figure 2.8: The original endoscopic images appearing at the left side and the corresponding spectrum images at the right side of the page. In these images, two different stages of cancer in the lungs are showed. [4]

In 2005, Novak and Hocenski [5] determine an acceptable method of texture feature extraction that could be used for a visual inspection of ceramic tiles quality shown in Figure 2.9. Traditional extraction of statistical features has been carried out as well as feature extraction based on local binary pattern(LBP). It operates in the neighborhood of eight pixels, using the value of the central pixel as a threshold. An LBP code of a particular neighborhood is calculated by assigning corresponding weights to every pixel and adding products.

First order statistical coefficients were less efficient. Since they do not have any pixel spatial structure information, but just the information on their values, we can conclude that for defect detection it is important to use features characterizing spatial relations between pixels. The second order statistical coefficients are almost identical and characterize homogeneity very well, since they did not make any false defect error in any case. All other methods include spatial structure information which in line with that show good results. The most efficient method of texture feature extraction is the method of a general rotation invariant and uniform LBP operator defined for 24 points distant form the central pixel for radius 3 (LBP_riu243). This method represents the first choice for a visual quality inspection system.

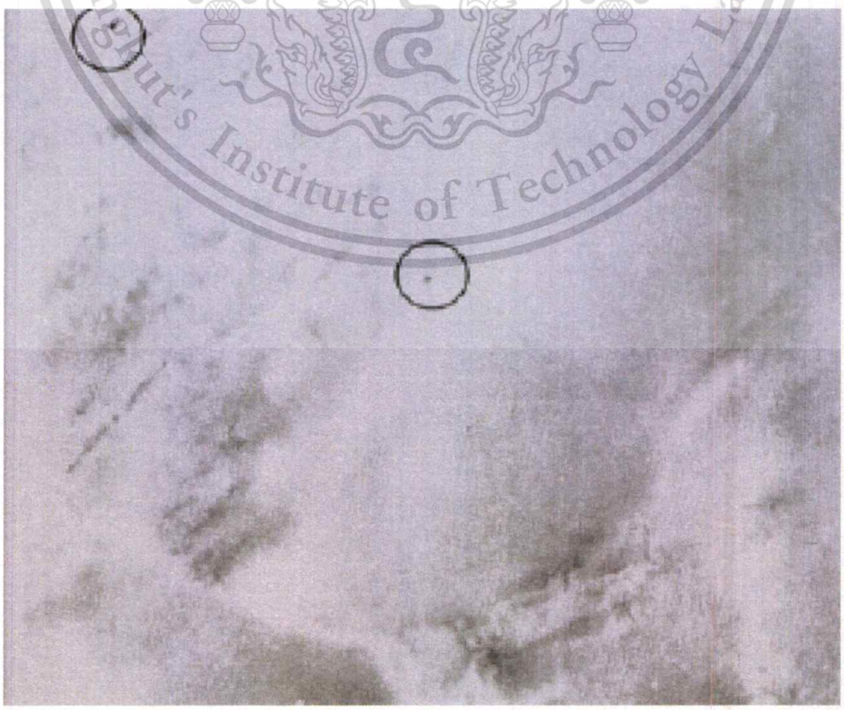

Figure 2.9: An example of ceramic tile with two defects. [5]

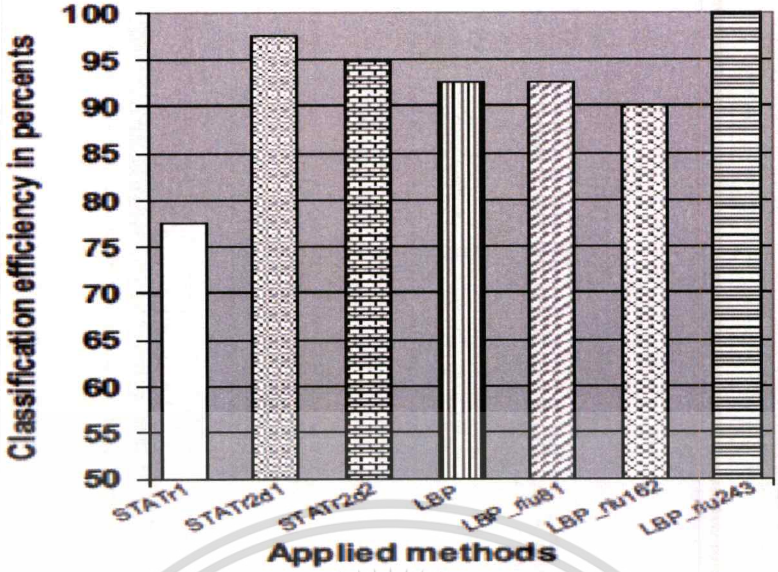

Figure 2.10: Comparison between various distances and various rotations of LBP. [5]

In 2006, Tomczak and Mosorov [6] proposed an algorithm for texture defects detection. The method doesn't require supervised classification. The algorithm can be simply applied to an automatic visual inspection system. For localization of texture defects features of each non-overlapping region of an image can be calculated via the Singular Value Decomposition (SVD) and image processing techniques. SVD is a widely used technique to decompose a matrix into several component matrices, exposing many of the useful and interesting properties of the original matrix. The algorithm uses the fuzzy c-means clustering (FCM) to classify each region into two clusters. FCM is a method of clustering which allows one piece of data to belong to two or more clusters. A distance between centers of defective and non-defective clusters using some threshold value is chosen empirically. The main advantage of the presented method over supervised classification methods is that it doesn't need to use training collection to realize texture defect detection.

Experimental results show that it is invariant to different sort of material textures and defects and it can be applied in the automatic systems realizing visual inspection of such materials as: wood, paper, rock or metal. As opposed to many other texture defect detection methods, the algorithm doesn't need a training set, consisting of material textures, which simplify its possible applying in an automatic visual inspection system.

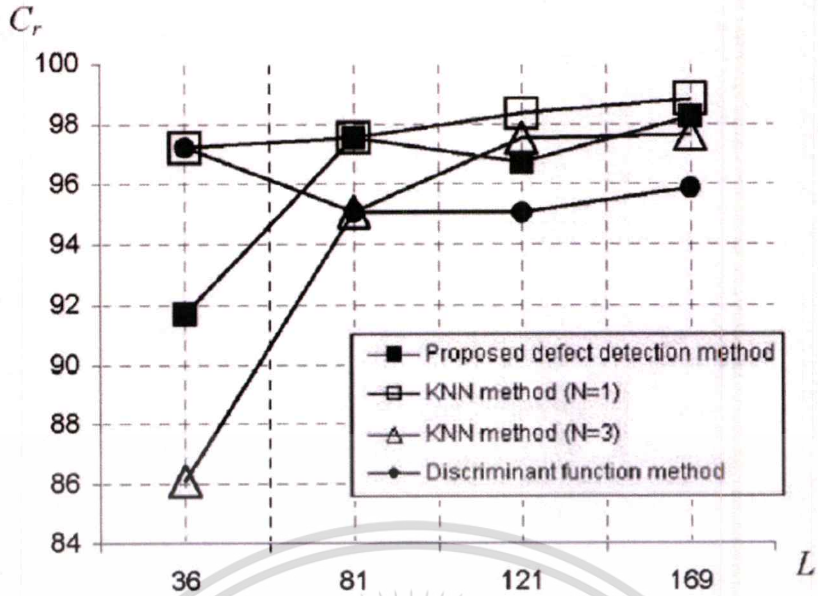

Figure 2.11: Recognition rates C_r calculated for defect detection method. [6]

In 2007, Tomczak and Mosorov [7] presented Two texture defect detection methods for automatic visual inspection systems; Principle Component Analysis (PCA) and SVD. The PCA technique determines the perpendicular axes (called eigenvectors). The eigenvector of the largest eigenvalue is the first principal component. The eigenvector of the second largest eigenvalue is the second principal component and so on. There will be the same number of axes as variables (dimensions), the longest axis is the First Principle Component (PC1), and next major axis is the Second Principle Component (PC2). Algorithm makes a slice through the cloud of data vectors using the 2-dimensional space defined by PCr, r=1,2 and projects all of the data vectors onto this space, then obtains a 2-dimensional representation of the data vectors retaining the maximum variation (information) contained in the multivariate data.

An analyzed texture image can be divided into non-overlapping samples, and then calculate features of each sample using statistical analysis. Finally, the clustering of those features is applied to recognize the sample as defective or non-defective. This methods do not require a previous training step to collect defective and non-defective texture samples. The experimental results show that these methods are effective and more accurate than earlier methods for image texture defect detection.

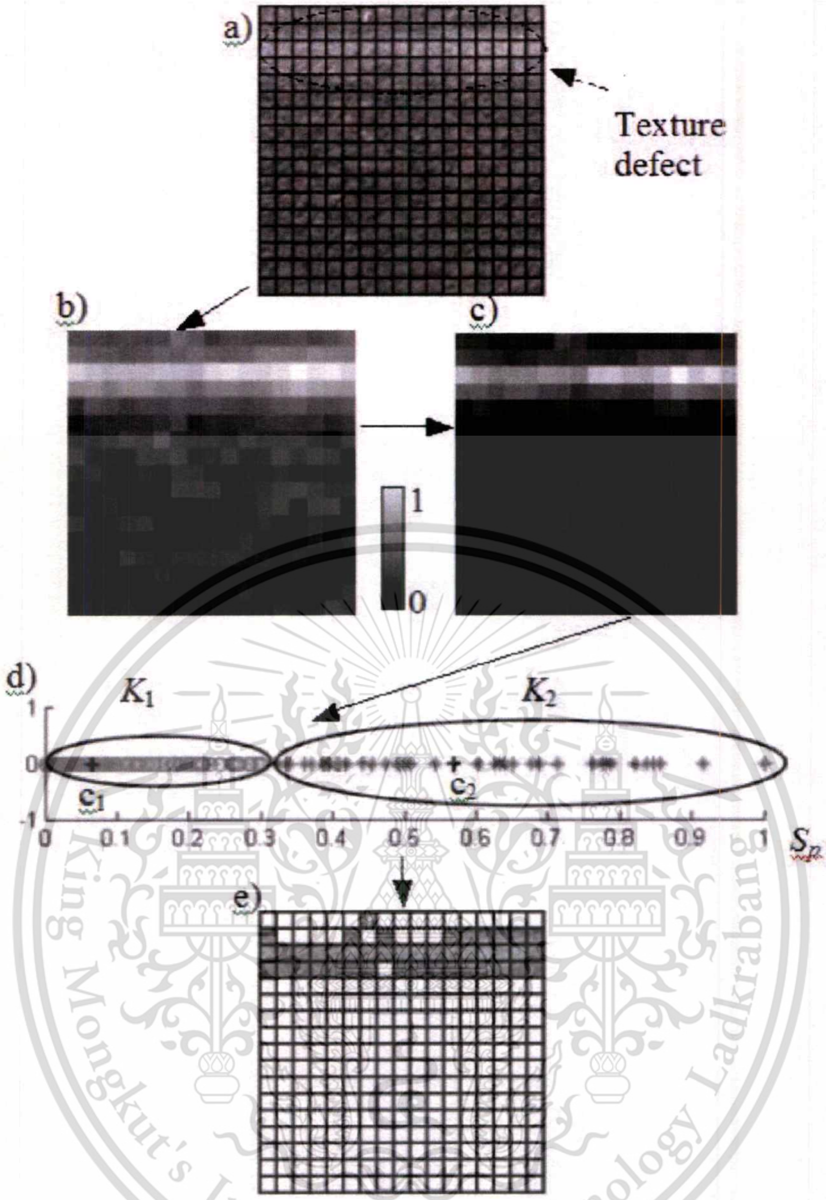

Figure 2.12: Steps of presented texture defect detection algorithm. [7]

Even though there are many images processing research on the defects detection on parts surface, but cannot find an algorithm in a public paper to detect the contamination on ABS at the HGA level, which need high resolution and fast processing time to support HDD industry.

In this thesis, we have developed algorithm for HDD industry on MATLAB to detect the contamination which is bigger than 5 micrometer on the ABS at the HGA level. Chapter3 presents the theory of slider fly height and image processing used in this thesis.

CHAPTER 3

THEORY

3.1 Contrast enhancement

The quality of an image as human can perceived could be improved by image enhancement techniques. This is because many ABS images when examined on a color display give inadequate information for image interpretation. There is no conscious effort to improve the fidelity of the image with regard to some ideal form of the image. There are various techniques for the improving of image quality, more commonly used were the stretch, density slicing, edge enhancement, and spatial filtering. The approach of image enhancement is attempted after the image is corrected for geometric and radiometric distortions. Thus, its methods were applied separately to each band of a multispectral image. Moreover, digital techniques have been found to be most satisfactory than the photographic technique for image enhancement, because of the precision and wide variety of digital processes.

Contrast generally refers to the difference in luminance or grey level values in an image and is an important characteristic. It can be defined as the ratio of the maximum intensity to the minimum intensity over an image. To the attempt of the resolving power and the ability of detectable of an image the contrast ratio has its strong bearing role. Larger on this ratio, more easily it is to interpret the image. Generally, ABS images lack adequate contrast and require contrast improvement.

Contrast enhancement techniques expand the range of brightness values in an image so that the particular image can be efficiently displayed in a manner desired by the analyst. The density values in a scene generally were pulled farther apart, that is, expanded over a greater range. The effect is to increase the visual contrast between two areas of different uniform densities. This approach enables the analyst to discriminate between areas initially having a small difference in density more easily.

3.1.1 Linear Mapping (Linear Point Operations)

The overall brightness of a gray-scale image can be adjusted by adding a constant bias, b, to pixel values:

$$g(x,y) = f(x,y) + b \tag{3.1}$$

The overall brightness of the image is increased if b>0 , and decreased if b<0 . An example to increasing and decreasing the brightness of an image is shown in Figure 3.1.

Figure 3.1: Image brightness. [8]

The contrast of a gray-scale image can be adjusted by multiplying all pixel values by a constant gain, a:

$$g(x,y) = af(x,y) \tag{3.2}$$

The overall contrast of the image is increased if a>1, and decreased if a<1. An example to increasing and decreasing the contrast of an image is shown in Figure 3.2.

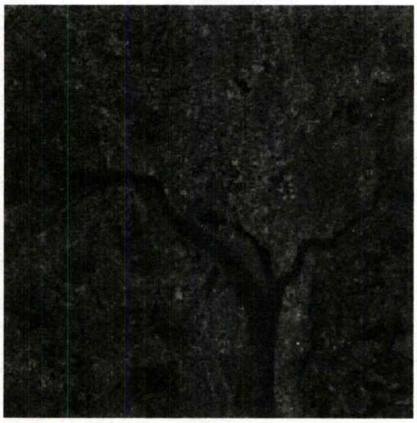

Original image

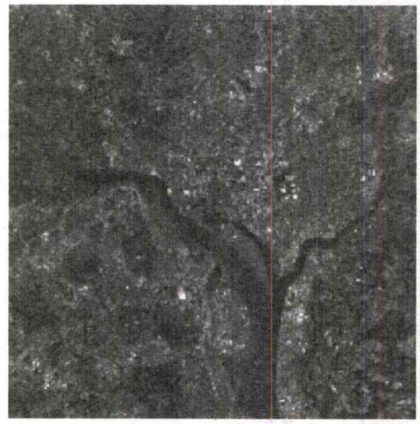

Result of multiplying pixel value by 2

Figure 3.2: Image contrast. [8]

Brightness and contrast equations can be combined to give a single expression for brightness and contrast adjustment:

$$g(x,y) = af(x,y) + b \tag{3.3}$$

3.1.2 Linear Contrast Stretch

This approach is the simplest contrast stretch algorithm. The grey values in the original image and the modified image follow a linear relation in this algorithm. A density number in the low range of the original histogram is assigned to extremely black and a value at the high end is assigned to extremely white. The remaining pixel values are distributed linearly between these extremes. The features or details that were obscure on the original image will be clear in the contrast stretched image. Linear contrast stretch operation can be represented graphically as shown in Figure 3.3. To provide optimal contrast and color variation in color composites the small range of grey values in each band is stretched to the full brightness range of the output or display unit.

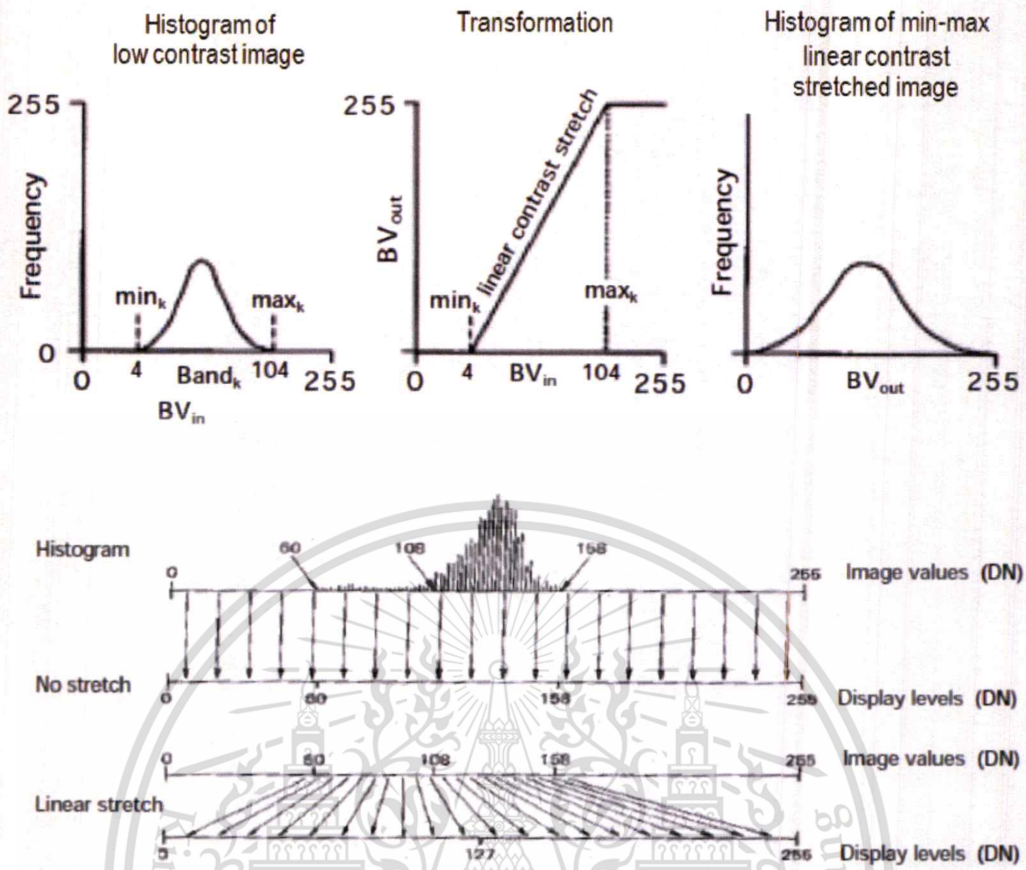

Figure 3.3: Linear contrast stretch (source Lillesand and Kiefer, 1993). [9]

A high-contrast image spans the full range of gray-level values. A low-contrast image can be transformed into a high-contrast image by remapping or stretching the gray-level values such that the histogram spans the full range. The contrast stretch is often referred to as the dynamic range adjustment (DRA). The simplest contrast stretch is a linear transform that maps the lowest gray level GLmin in the image to zero and the highest value GLmax in the image to 255 (for an eight-bit image), with all other gray levels remapped linearly between zero and 255, to produce a high-contrast image that spans the full range of gray levels. This linear transform is given by

$$g'(x,y) = INT\left\{\frac{255}{GL_{\max} - GL_{\min}}\left[g(x,y) - GL_{\min}\right]\right\} \tag{3.4}$$

Where the INT function returns the integer value. If we wish to remap the image to a gray-level range defined by a new minimum GL′min and a new maximum defined by GL′max, the linear transform (Figure 3.4) can be generalized to

$$g'(x,y) = INT\left\{\frac{GL'_{\max} - GL'_{\min}}{GL_{\max} - GL_{\min}}\left[g(x,y) - GL_{\min}\right] + GL'_{\min}\right\} \tag{3.5}$$

The linear transform for contrast enhancement spreads the gray-level values evenly over the full contrast range available; thus, the relative shape of the histogram still remains unchanged but is widened to fill the range. The stretching of the histogram creates evenly distributed gaps between gray-level values in the image. Although the linear transform will increase the contrast of the image, the steps between the populated gray-level values increase in contrast as well, which can resulted in visible contouring artifacts in the image (Figure 3.5).

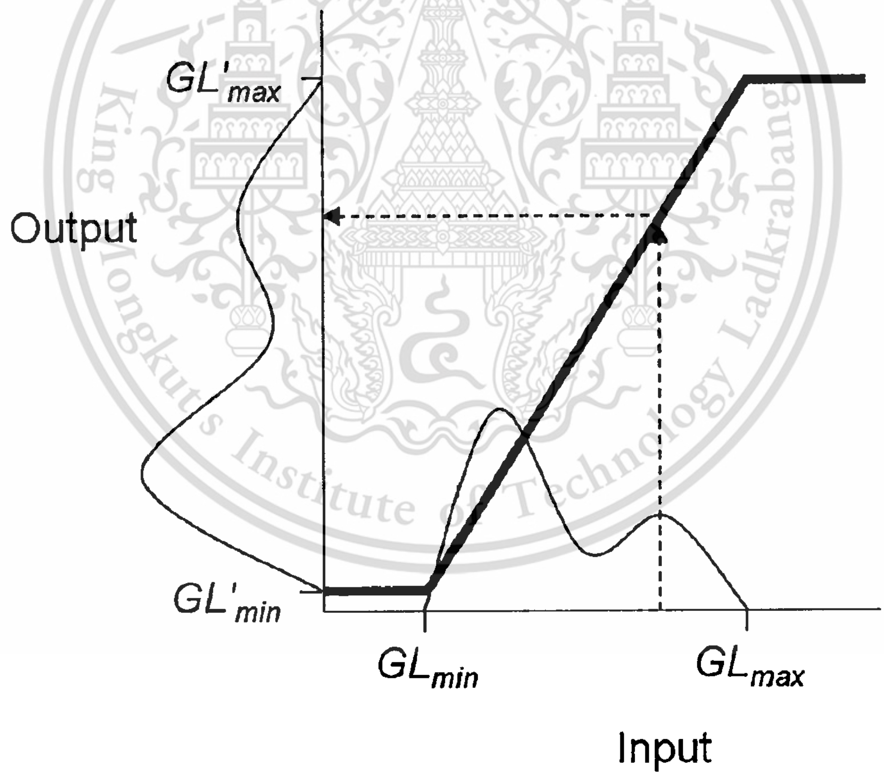

Figure 3.4: A Linear transform that remaps the gray levels between GL′min and GL′max

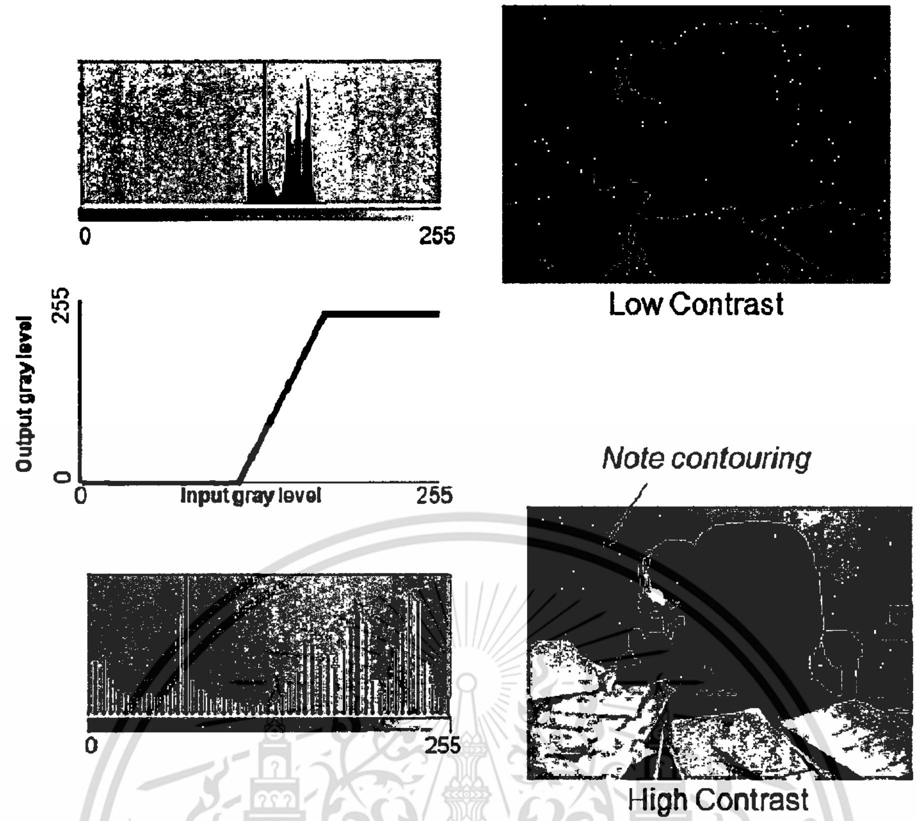

Figure 3.5: Enhancement of low-contrast images can produce image artifacts. [10]

Additional contrast enhancement can be achieved if replace GLmin and GLmax in Eq. (3.5) with points that penetrate the gray-level histogram, with Pmin > GLmin penetrating the low end and Pmax < GLmax penetrating the high end. The gray-level transform is then given by

$$g'(x,y) = INT\left\{\frac{GL'_{max} - GL'_{min}}{P_{max} - P_{min}}\left[g(x,y) - P_{min}\right] + GL'_{min}\right\} \tag{3.6}$$

If GL′min = 0 and GL′max = 255, then the gray levels between GLmin and Pmin will be clipped to zero and the gray levels between Pmax and GLmax will be clipped to 255, but this may be a valid compromise to get the additional enhancement.

A useful calculation to help determine the best penetration points is the cumulative histogram, which is generated by finding the total number of pixels in the gray-level histogram between zero and each gray level. If the gray-level histogram is given by P(GL), the cumulative histogram is given by

$$P_{cumm}(GL) = \sum_{i=0}^{GL} P(i) \tag{3.7}$$

The values for Pmin and Pmax can be calculated for each image using predefined percentages of the cumulative histogram that will be clipped to zero and 255. The gray-level histogram P'(GL) of the processed image will cover the full contrast range but will also have more pixels at zero and 255 due to the clipping.

3.1.3 Non-Linear Contrast Enhancement

For this approach, the input and output data values follow a non-linear transformation. The general form of the non-linear contrast enhancement is defined by y = f (x), where x is the input data value and y is the output data value. The non-linear contrast enhancement techniques have been found to be useful for the process of enhancing the color contrast between the nearly classes and subclasses of a main class.

A type of non-linear contrast stretch involves scaling the input data logarithmically. This enhancement has greatest impact on the brightness values found in the darker part of histogram. It could be reversed to enhance values in brighter part of histogram by scaling the input data using an inverse log function.

Histogram equalization is another non-linear contrast enhancement technique. In this technique, histogram of the original image is redistributed to produce a uniform population density. This is obtained by grouping certain adjacent grey values. Thus the number of grey levels in the enhanced image is less than the number of grey levels in the original image.

3.2 Statistics

Statistics method based on the analyzing of particular big set of data, in order to find the relationships between the individual points in that data set. There is various methods to measure with the set of data which could demonstrate what is the data result can be given.

3.2.1 Standard Deviation

To understand standard deviation, a data set is indeed requires. Statisticians are usually concerned with taking a sample of a population. Election polls as an example, the population is all the people in the country, whereas a sample is a subset of the population that the statisticians measure. The great thing about statistics is that by only measuring a sample of the population, for example by a phone call survey, it is most likely to be the measurement if used the entire population. In this statistics section, assuming that the particular data sets are samples of some bigger population. There are a number of things can be calculate about a data set. For example, to calculate the mean of the sample with below given the formula:

$$\bar{X} = \frac{\sum_{i=1}^{n} X_i}{n} \tag{3.8}$$

The Standard Deviation (SD) of a data set is a measure of how spread out the data is. The English definition of the SD is: "The average distance from the mean of the data set to a point". The way to calculate it is to compute the squares of the distance from each data point to the mean of the set, add them all up, divide by n-1 , and take the positive square root. As a formula:

$$SD = \sqrt{\frac{\sum_{i=1}^{n} \left(X_i - \bar{X}\right)^2}{(n-1)}} \tag{3.9}$$

3.2.2 Variance

Variance is another measurement of the spread of data in a data set. In fact it is almost identical to the standard deviation. The formula is below:

$$SD^2 = \frac{\sum_{i=1}^{n}\left(X_i - \bar{X}\right)^2}{(n-1)} \tag{3.10}$$

It can be noticed that this is simply the standard deviation squared, in both the symbol (SD^2) and the formula (there is no square root in the formula for variance). SD^2 is the usual symbol for variance of a sample. Both these measurements are measures of the spread of the data. Standard deviation is the most common measure, but variance is also used in many circumstances. Above explanation of variance in addition to standard deviation is to provide a solid platform from which the next section, covariance, can launch from.

3.2.3 Covariance

Standard deviation and variance only operate on 1 dimension. The resulted were only to calculate the standard deviation for each dimension of the data set independently of the other dimensions. However, it is useful to have a similar measure to find out how much the dimensions vary from the mean with respect to each other.

Covariance is such a measure. Covariance is always measured between 2 dimensions. If it is use to calculate the covariance between one dimension and itself, resulted is the variance. So, if a calculation is at a 3-dimensional data set (x , y , z), then the measure of the covariance between the x and y dimensions, the x and z dimensions, and the y and z dimensions can be operate. To measuring the covariance between x and x , or y and y , or z and z would given the variance of the x , y and z dimensions respectively.

The formula for covariance is very similar to the formula for variance. The formula for variance could also be written per below:

$$\operatorname{var}(X)=\frac{\sum_{i=1}^{n}(X_i-\bar{X})(X_i-\bar{X})}{(n-1)} \tag{3.11}$$

where can simply expanded the square term to show both parts. So given that knowledge, here is the formula for covariance:

$$\operatorname{cov}(X,Y)=\frac{\sum_{i=1}^{n}(X_i-\bar{X})(Y_i-\bar{Y})}{(n-1)} \tag{3.12}$$

If the covariance is positive, then that indicates that both dimensions increase together. If the value is negative, then as one dimension increases, the other decreases. In the last case, if the covariance is zero, it indicates that the two dimensions are independent of each other. However, the luxury of being able to visualize data is only available at 2 and 3 dimensions. Since the covariance value can be calculated between any 2 dimensions in a data set, this technique is often used to find relationships between dimensions in high-dimensional data sets where visualization is difficult.

3.2.4 The covariance Matrix

Covariance is always measured between 2 dimensions. If the subject of measurement is a data set with more than 2 dimensions, there is more than one covariance measurement that can be calculated. For example, from a 3 dimensional data set (dimensions x , y , z) it can calculate cov(x,y), cov(x,z) and cov(y,z). In fact, for an n-dimensional data set, it can calculate $\frac{n!}{(n-2)!\times 2}$ different covariance values.

A useful way to get all the possible covariance values between all the different dimensions is to calculate them all and put them in a matrix. So, the definition for the covariance matrix for a set of data with n dimensions is:

$$C^{n\times n}=\left(c_{i,j}, c_{i,j}=\operatorname{cov}(Dim_i, Dim_j)\right) \tag{3.13}$$

where $C^{n\times n}$ is a matrix with n rows and n columns, and Dim_x is the xth dimension. if the subject have an n-dimensional data set, then the matrix has n rows and columns (so is square) and each entry in the matrix is the result of calculating the covariance between two separate dimensions. For example, the entry on row 2, column 3, is the covariance value calculated between the 2nd dimension and the 3rd dimension.

If made up the covariance matrix for an imaginary 3 dimensional data set, using the usual dimensions x , y and z . Then, the covariance matrix has 3 rows and 3 columns, and the values are this below:

$$C=\begin{pmatrix} \operatorname{cov}(x,x) & \operatorname{cov}(x,y) & \operatorname{cov}(x,z) \\ \operatorname{cov}(y,x) & \operatorname{cov}(y,y) & \operatorname{cov}(y,z) \\ \operatorname{cov}(z,x) & \operatorname{cov}(z,y) & \operatorname{cov}(z,z) \end{pmatrix} \tag{3.14}$$

Note: Down the main diagonal, the covariance value is between one of the dimensions and itself. These are the variances for that dimension. The other point is that since $\operatorname{cov}(a,b)=\operatorname{cov}(b,a)$, the matrix is symmetrical about the main diagonal.

3.3 Matrix Algebra

This section objective aims to provide a background for the matrix algebra required in PCA, specifically through at eigenvectors and eigenvalues of a given matrix.

Eigenvectors and eigenvalues are numbers and vectors associated to square matrices. Together they provide the eigen-decomposition of a matrix, which analyzes the structure of this matrix. Even though the eigen-decomposition does not exist for all square matrices, it has a particularly simple expression for matrices such as correlation, covariance, or cross-product matrices. The eigen-decomposition of this type of matrices is to be clarify as significant factor because it is used to find the maximum (or minimum) of functions involving these matrices. Especially PCA is obtained from the eigen-decomposition of a covariance or a correlation matrix.

There are several ways to define eigenvectors and eigenvalues, the most common approach defines an eigenvector of the matrix A as a vector u that satisfies the following equation:

$$\mathrm{A}u = \lambda u \tag{3.15}$$

When rewritten, the equation becomes:

$$(\mathrm{A} - \lambda \mathrm{I})u = 0 \tag{3.16}$$

where λ is a scalar called the eigenvalue associated to the eigenvector. In a similar manner, it can be also clarify that a vector u is an eigenvector of a matrix A if the length of the vector (but not its direction) is changed when it is multiplied by A.

To solve the eigenvalue problem for an n by n matrix, below steps can be follow;

1. Compute the determinant of $\mathrm{A} - \lambda \mathrm{I}$. With λ subtracted along the diagonal, this determinant starts with λ^n or $-\lambda^n$. It is a polynomial in λ of degree n.
2. Find the roots of this polynomial, by solving $\det(\mathrm{A} - \lambda \mathrm{I}) = 0$. The n roots are the n eigenvalues of A. They make $\mathrm{A} - \lambda \mathrm{I}$ singular.
3. For each eigenvalue λ, solve $(\mathrm{A} - \lambda \mathrm{I})x = 0$ to find an eigenvector x.

More detail calculate can be found in Appendix B.

3.4 Principal Components Analysis (PCA)

Principal Components Analysis (PCA) is a method to identify patterns in data, and express the data in a way to highlight their similarities and dissimilarities. In other describable it is a numerical procedure for analyzing the basis of variation present in a multi-dimensional data set. PCA has been called one of the most valuable results from applied linear algebra. It is used in all forms of analysis - from neuroscience to computer graphics and image compression - because it is a simple, non-parametric method of extracting significant information from confusing data sets. With least additional effort PCA provides a roadmap for how to shrink a complex data set to a lower dimension to disclose the hidden, simplified dynamics that often lie behind it. An essential difficulty to experimental science is that the data appears unclear and redundant. Examples abound from complex systems such as neuroscience, photo-science, meteorology and oceanography.

3.4.1 Goals of PCA

The goals of PCA are as follows;

1. Extract the most important information from the data table.
2. Compress the size of the data set by keeping only this important information.
3. Simplify the description of the data set.
4. Analyze the structure of the observations and the variables.

3.4.2 Method

Step 1: Get some data

For example, to use 2-dimensional data;

$$\text{Data} = \begin{array}{c|c} x & y \\ \hline 2.5 & 2.4 \\ 0.5 & 0.7 \\ 2.2 & 2.9 \\ 1.9 & 2.2 \\ 3.1 & 3.0 \\ 2.3 & 2.7 \\ 2 & 1.6 \\ 1 & 1.1 \\ 1.5 & 1.6 \\ 1.1 & 0.9 \end{array}$$

Figure 3.6: Example data

Step 2: Subtract the mean

To aims for the PCA to works appropriately, it should goes by subtract the mean from each of the data dimensions. The mean subtracted is the average across each dimension. So, all the x values have x bar (the mean of the x values of all the data points) subtracted, and all the y values have y bar subtracted from them. This produces a data set whose mean is zero.

Step 3: Calculate the covariance matrix

Since the data is 2 dimensional, the covariance matrix will be 2 x 2. For example, assuming the covariance matrix is:

$$\mathrm{cov} = \begin{pmatrix} 0.616556 & 0.615444 \\ 0.615444 & 0.716556 \end{pmatrix} \tag{3.17}$$

Since the non-diagonal elements in this covariance matrix are positive, it can be expect that both the x and y variable increase together.

Step 4: Calculate the eigenvectors and eigenvalues of the covariance matrix

Since the covariance matrix is square, it can be calculate the eigenvectors and eigenvalues for this matrix. Below are the eigenvectors and eigenvalues:

$$eigenvalues = \begin{pmatrix} 0.049083 \\ 1.284028 \end{pmatrix} \tag{3.18}$$

$$eigenvectors = \begin{pmatrix} -0.735179 & -0.677873 \\ 0.677873 & -0.735179 \end{pmatrix} \tag{3.19}$$

For PCA the unit eigenvectors were requires. Eigenvectors provide the information about the patterns in the data, considering these eigenvectors are perpendicular.

If draw the data points, the result is that one of the eigenvectors goes throughout the middle of the point. That eigenvector is showing how these two data sets are related along that line. The second eigenvector gives us the other, less significant, pattern in the data.

So, by this process of taking the eigenvectors of the covariance matrix, it can be able to extract lines that characterize the data. The rest of the steps involve transforming the data so that it is expressed in terms of them lines.

Step 5: Choosing components and forming a feature vector

Here is where the notion of data compression and reduced dimensionality comes into it. If going through at the eigenvectors and eigenvalues from the previous section, it can be notice that the eigenvalues are quite different values. In fact, it turns out that the eigenvector with the highest eigenvalue is the principle component of the data set.

In the mentioned example, the eigenvector with the largest eigenvalue was the one that pointed down the middle of the data. It is the most significant relationship between the data dimensions.

In general, once eigenvectors are found from the covariance matrix, the next step is to order them by eigenvalue, highest to lowest. This gives the components in order of significance. The ignorance to the components of lesser significance also can be performed. Some information might be lost, but if the eigenvalues are small, it does not much huge lost. If the process leave out some components, the final data set will have less dimensions than the original. To be precise, if have n dimensions in the data originally, then it can be to calculate n eigenvectors and eigenvalues, and then choose only the first p eigenvectors. Finally, the final data set has only p dimensions.

What needs to be done now is the needed to form a feature vector, or as referred for a matrix of vectors. This is constructed by taking the eigenvectors that in order to keep from the list of eigenvectors, and forming a matrix with these eigenvectors in the columns.

$$FeatureVector = \begin{pmatrix} eig_1 & eig_2 & eig_3 & .... & eig_n \end{pmatrix} \tag{3.20}$$

Given example set of data, and the fact that now 2 eigenvectors are appears, it could generate as two choices, either to form a feature vector with both of the eigenvectors:

$$\begin{pmatrix} -0.677873 & -0.735179 \\ -0.735179 & 0.677873 \end{pmatrix}$$

or, to leave out the smaller, less significant component and only have a single column:

$$\begin{pmatrix} -0.677873 \\ -0.735179 \end{pmatrix}$$

Step 6: Deriving the new data set Final step in PCA, and is also the easiest. Once had been chosen of the components (eigenvectors) that wish to keep in the data and formed a feature vector, it can be simply to take the transpose of the vector and multiply it on the left of the original data set, transposed.

$$FinalData = RowFeatureVector \times RowDataAdjust \tag{3.21}$$

Where RowFeatureVector is the matrix with the eigenvectors in the columns transposed so that the eigenvectors are now in the rows, with the most significant eigenvector at the top, and RowDataAdjust is the mean-adjusted data transposed, that is, the data items are in each column, with each row holding a separate dimension, where FinalData is the final data set, with data items in columns, and dimensions in rows.

PCA will given the original data exclusively in form of the vectors had been chose. The original data set mentioned had two axes, x and y, so this particular data was in form of them. The expression is the most efficient when the axes are perpendicular. This was the reason why it was important that eigenvectors are always perpendicular to each other.

Basically what the process have done here was that to transformed the data so that is expressed in terms of the patterns between them, where the patterns are the lines that most strongly describe the relationships between the data

3.4.3 Summary of Assumptions and Limits

In this part it will provide as an important context for the understanding when PCA does not work properly and also an introduction to new extensions of PCA.

1. Linearity

Linearity outlines the problem as a change of basis. Several research areas have investigated the ways to apply a non-linearity prior to PCA which could extend this algorithm. This extension of PCA has been expressed as kernel PCA.

2. Mean and variance are adequate statistics

Assumed that the mean and the variance completely express a probability distribution. The only zero-mean probability distribution that is entirely described by the variance is the Gaussian distribution.

3. Large variances have significant dynamics

This assumption consists of the belief that the data has a high SNR (Signal to Noise Ratio). Therefore, principal components with larger related variances characterize interesting dynamics, while those with lower variances represent noise.

4. Orthogonal Principal Components

This assumption provides an intuitive generalization that makes PCA solvable with linear algebra decomposition methods.

Assumptions and limits presented here in this chapter are globally assumed throughout all next chapters.

CHAPTER 4

RESEARCH METHODOLOGY

4.1 Vision system design

This section represents as a brief description of the imaging system used to register the ABS area. It is necessary to consider all the parameters relevanted to select the most appropriate industrial CCD camera. The ABS samples are very tiny with their size no larger than 1.5 by 1 mm. Therefore, the field of view (FOV) must be set accordingly. Furthermore, a contamination can be as small as 5 μm., and this defines the resolution limit of the imaging system.

From the given information, it is possible to calculate the minimum pixel dimension, N_{pix}.

$$N_{pix} = 2 * d_{FOV} / \delta \tag{4.1}$$

N_{pix} (Hor.) = 2 * 1.5 / 0.005 = 600 pixels

N_{pix} (Ver.) = 2 * 1 / 0.005 = 400 pixels

where d_{FOV} is the width or height of the FOV, and δ is the resolution limit or the smallest feature that needs to be resolved. Thus, from this equation, the horizontal and vertical dimensions of the CCD sensor must be at least 600 and 400 pixels, respectively, in order to capture the entire FOV with sufficient details. This specification matches a commercially available CCD sensor that has dimensions of 1392 by 1040 pixels and white coaxial light for our vision system. The getting of input images from camera will not be detailed in this research.

4.2 Algorithm development

The image processing algorithm proposed in this thesis comprises three major steps: Extraction of Region of Interest (ROI), Image preprocessing by contrast enhancement, and clustering defected and non-defected by PCA. In this research, the ABS contains inequity surfaces which each had generated in separate parts. Thus, the analyzing cannot be done simultaneously. It is necessary to determine the ROI of the ABS. While the image preprocessing is sensitive enough to pick up even tiny contamination, other irrelevant regions could be mistakenly included as well. Hence, in order to increase the specificity of the algorithm, at the final stage some rules are used to discriminate the possible contamination regions by PCA. The proposed algorithm was developed in the MATLAB R2012a.

4.2.1 Extraction of ROI

Mentioned before in the introduction section, air passing under the air bearing surfaces (ABS) provide the required "lift" and their design has to take into account the weight, velocity, and skew to achieve a uniformed flying height. From this requirement, the ABS surfaces contain difference steps, by those inequity steps, had created variety pattern on the surface itself distinguished the ABS surface into portions. In this research, researcher had taken some portion of the ABS to analyze by cropping in quadrate area 64 x 64 pixels for total 4 ROI per 1 ABS, as shown in Figure 4.1.

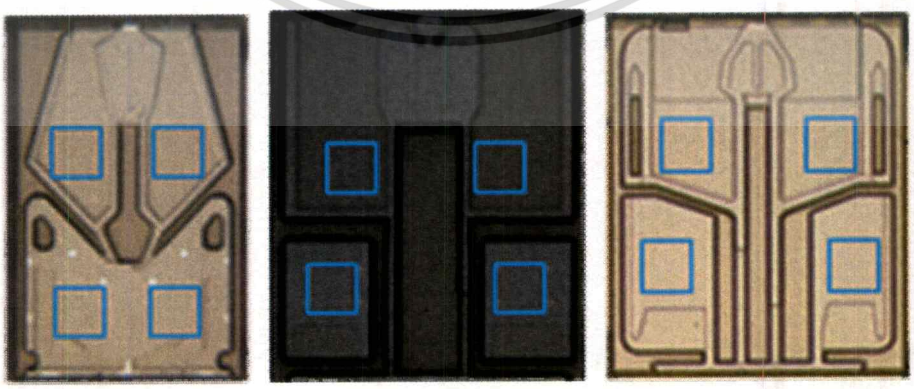

Figure 4.1: Three models of sample images.
Region of Interest has shown in rectangle.

Image from the cropping method still contains in RGB images. Therefore, to have an easier analyzing, researcher had converts RGB images to grayscale by elimination the hue and saturation information while retaining the luminance.

4.2.2 Image preprocessing by contrast enhancement

After the processing of ROI Extraction, now will result the image which contains 64X64 pixels grayscale and ready for next progress of the preprocessing image. In this research, the Contrast Enhancement is used.

Contrast Enhancement is an image enhancement technique that maps an image's contrast values to a new range. If done remapping the data values to fill the entire intensity range between 0 and 255, the contrast of the image can be increased. For this Contrast enhancement method, it allows to set the value for a new range. Moreover, the adjusting of Gamma correction value also can be employed. Depending on the value of gamma, the mapping between values in the input and output images might be nonlinear. Gamma can be any value between 0 and infinity. If gamma is 1, the mapping is linear. If gamma is less than 1, the mapping is weighted toward brighter. If gamma is greater than 1, the mapping is weighted toward darker. Figure 4.2 shows three different gamma correction settings.

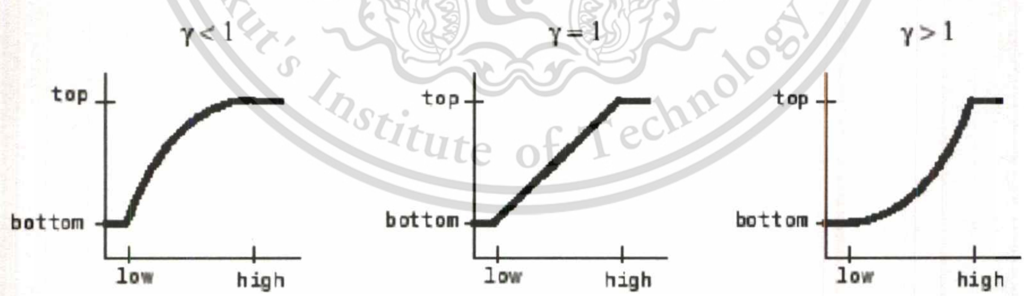

Figure 4.2: Three different Gamma correction setting

In this research, a new range of data has been expanded to the maximum from 0 to 255 and the value of Gamma correction has been set at 1 for linear transformation. Thereafter, the image which has possessed the contrast enhancement will be re-adjusted to 1-dimension by creating histogram.

Histograms show the distribution of data values across a data range. They do this by dividing the data range into a certain number of intervals, tabulating the number of values that fall into each interval, and plotting the values in the bins using bars or wedges of varying height. From the changed into histogram, now it results that 1-dimensional data have gained are incompleted for each data range affected to the analyzing. However, in the next section, the interpolation will be used to complete the data in every range from 0 to 255.

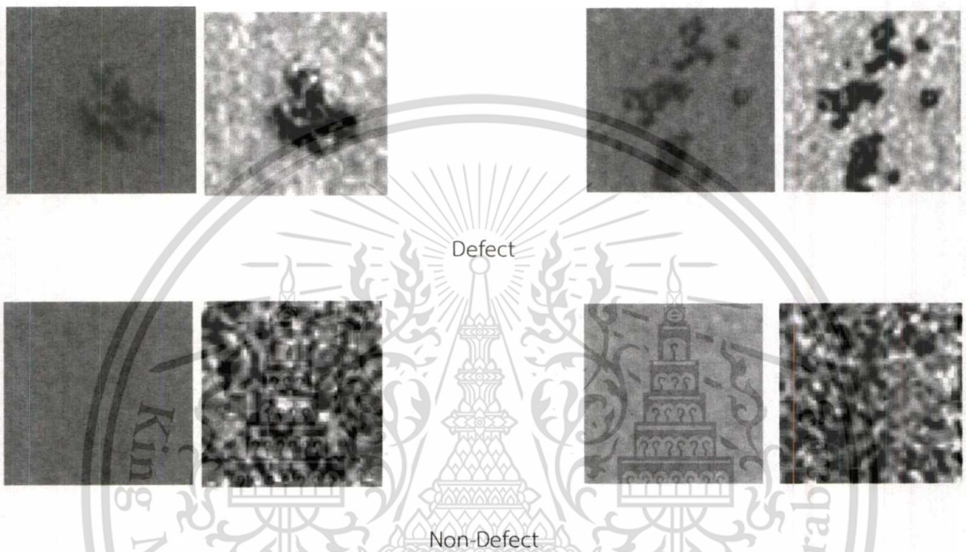

Figure 4.3: Contrast Enhancement Image

Interpolation is a method for estimating the value at a query location that within the domain of a set of data points. Table 4.1 shows various type of interpolation methods. The type of interpolation to be used are depended on the characteristics of the data being fit, the required smoothness of the curve, speed considerations, post-fit analysis requirements, and so on. The linear and nearest neighbor methods are faster way, but the resulting curves are not very smooth. The cubic spline and shape-preserving methods are slower, but the resulting curves are very smooth. In this research, Cubic spline is used.

Table 4.1: Interpolate methods

Method	Description
Linear	Linear interpolation: This method fits a different linear polynomial between each pair of data points for curves, or between set of three points for surfaces.
Nearest neighbor	Nearest neighbor interpolation: This method sets the value of an interpolated point to the value of the nearest data point. Therefore, this method does not generate any new data points.
Cubic spline	Cubic spline interpolation: This method fits a different cubic polynomial between each pair of data points for curves, or between sets of three points for surface.
Shape-preserving	Piecewise cubic Hermite interpolation (PCHIP): This method preserves monotonicty and the shape of the data. For curves only.

4.2.3 Clustering defected and non-defected by PCA

After interpolation, full range 1-dimensional data will be analyzed by PCA. This useful technique can use to reduce the dimensionality of large data sets. PCA can also use to find signal in noisy data. This method generates a new set of variables, called principal components. Each principal component is a linear combination of the original variables. All the principal components are orthogonal to each other, so there is no redundant information. The principle components as a whole form an orthogonal basis for the space of the data. The full set of principle components is as large as the original set of variables. But it is commonplace for the sum of the variances of the first few principal components to exceed more than 80% of the total variance of the original data.

In this research, PCA method were described earlier in Chapter 3 and briefly summarized by Figure 4.4.

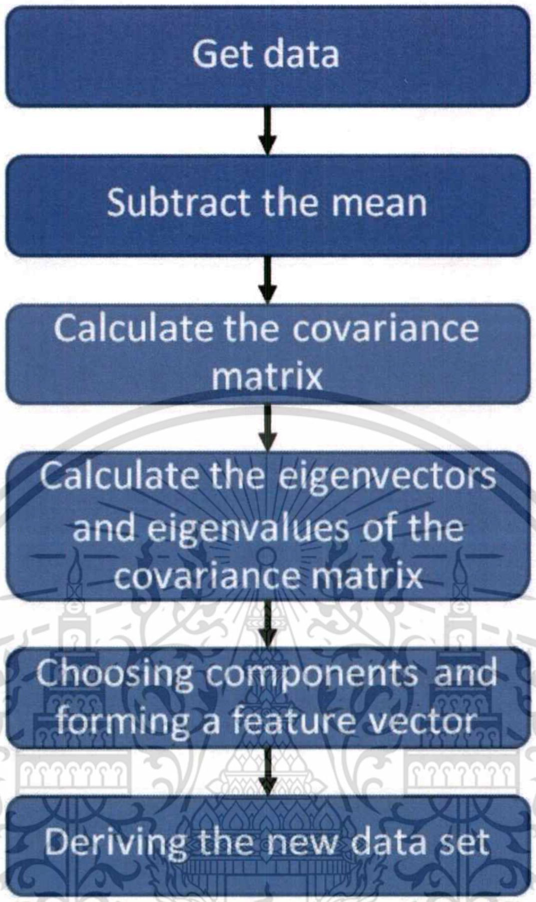

Figure 4.4: PCA Method

First and second principle components are used to cluster defect and non-defect. The first principle component is a single axis in space and the second principle component is another axis in space, perpendicular to the first as shown in Figure 4.5 - 4.6. Results of this research findings will be presented in the next chapter.

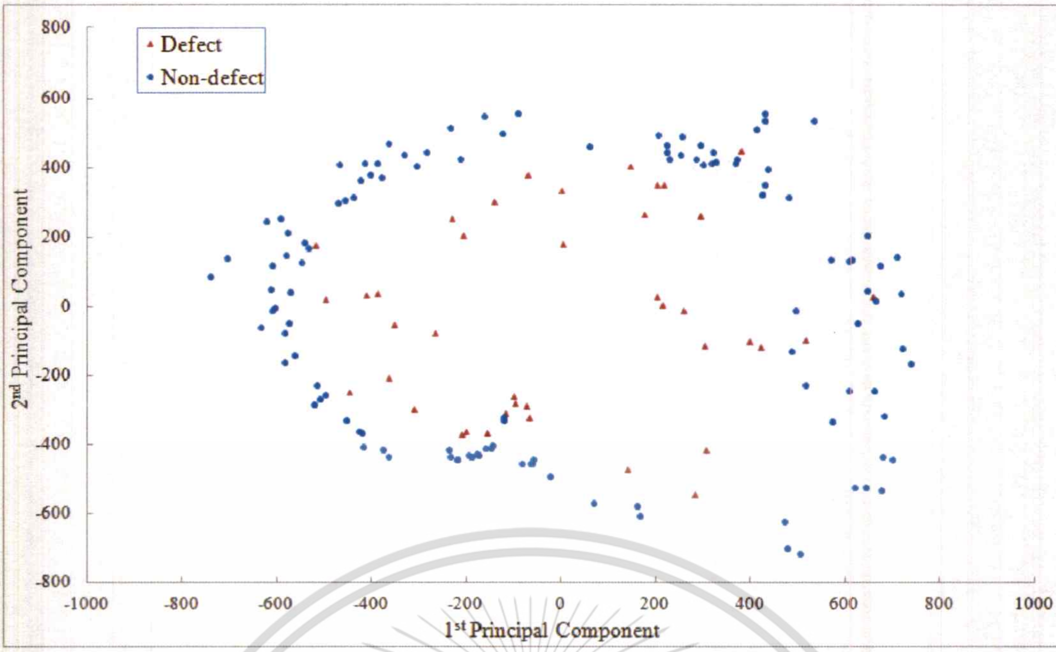

Figure 4.5: Two principal components without contrast enhancement

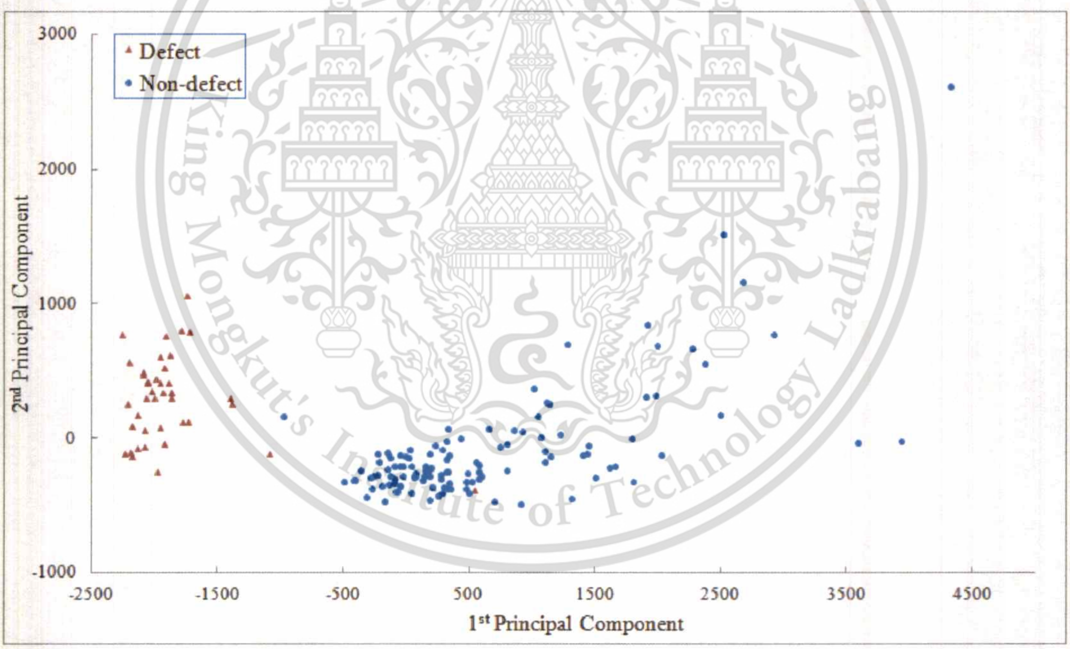

Figure 4.6: Two principal components with contrast enhancement

CHAPTER 5

RESULTS

In the experiment, the ABS images were collected by using the 1.3 megapixel camera. The sample ROI is a collection of 40 images from three ABS models as shown in Figure 5.1 for 4 ROI per an ABS. There were 160 ROI samples used to test our algorithm. The proposed method was implemented in the MATLAB R2012a. The experimental results will be discussed in two phases which are Image preprocessing phase and clustering defect and non-defect phase.

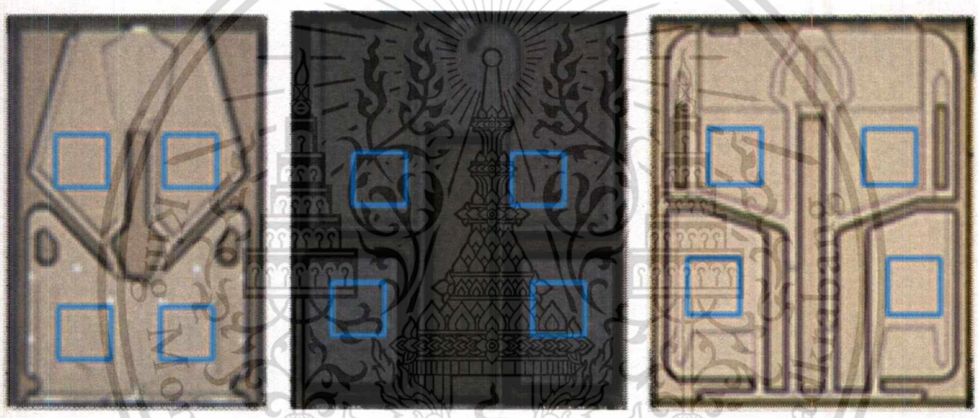

Figure 5.1: Three models of sample images.
Region of Interest has shown in rectangles.

From Figure 5.2, the comparison between image without contrast enhancement and image with contrast enhancement show the difference quality of an image. Thus, it can distinguish each image which leads to more efficient indication of non-defected images and defect images. ABS are made of Aluminium oxide and Titanium nitride. Under the higher expand range microscope, the texture of an ABS surface and also the grain can be visibly seen. Moreover, after the contrast enhancement processing, the image will be resulting in white and black alternating in every areas. Areas where the subjects are contaminated are shown as color of the contamination which are darker than the texture. Furthermore, the image will be resulted as 2 colors, the white as texture and the black as contamination.

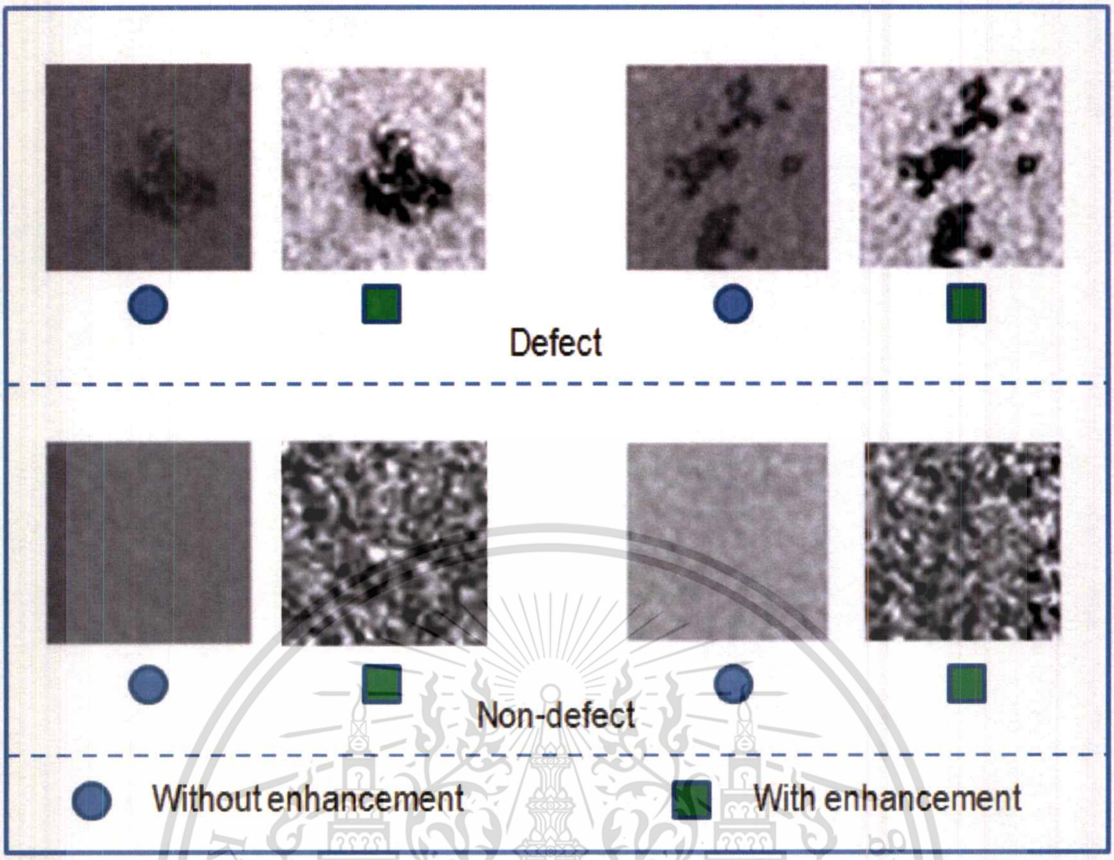

Figure 5.2: Contrast enhancement Image

When analyzed the image histogram in Figure 5.3 is analyzed the characteristic of data distribution are difference between non-defected and defected histogram. Non-defected histogram contains the groups of data in particular range, on the other hand, the defected histogram contains wider distribution of the data. However, either defected histogram or non-defected histogram for any images without Contrast enhancement possessed shows different mean. After running contrast enhancement, analysis of non-defected and the defected one are clearer. Furthermore, mean of each image of non-defected are similar.

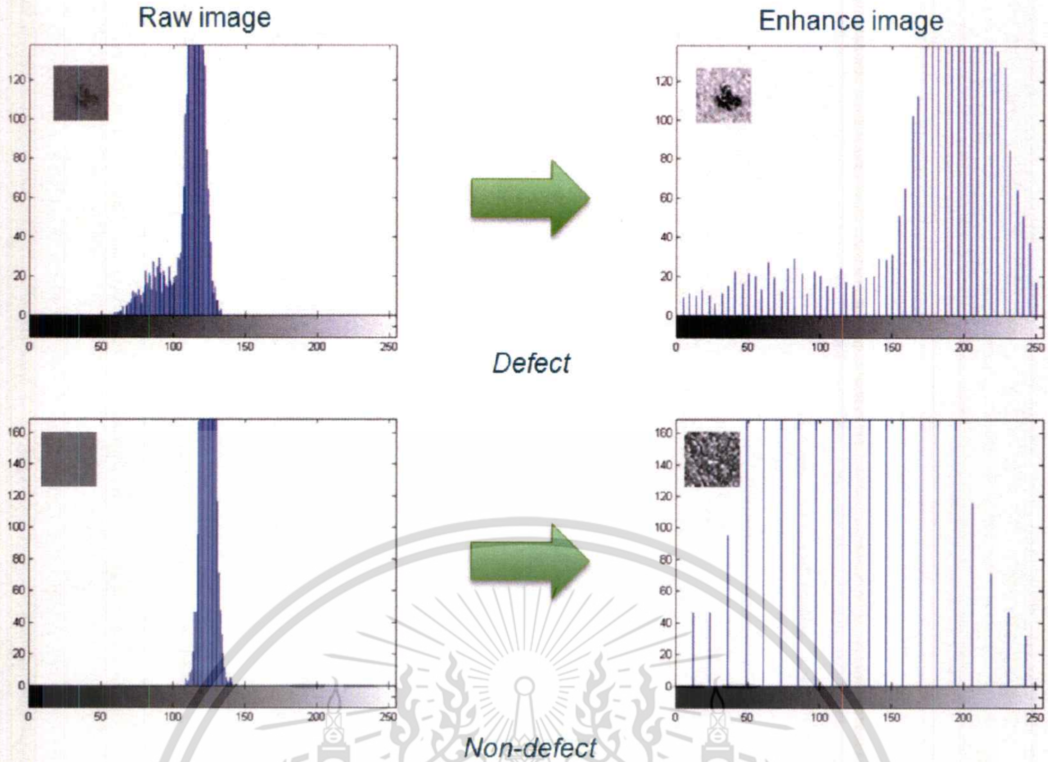

Figure 5.3: Histograms of detect and non-defect

Using the two principle components is possible for clustering defected and non-defected ABS. The sum of the variances of the first and second principal components are 54.10 % and 95.34 % of the total variance of the image data with and without contrast enhancement. However, principle component without image enhancement is not good enough for clustering defected and non-defected ABS. This is because the plot is sparse as shown in Figure 5.4. Figure 5.5 is the graph between PC1 and PC2 of the images possessed contrast enhancement method resulted the more visible distribution of data.

Selected thresholds in Figures 5.6 and 5.8 can be calculated from equation

$$\eta = \min\left(e_1 + e_2\right) \tag{5.1}$$

Where e_1 and e_2 are percentage of false rejection and false acceptance respectively. And η is a presetting threshold value for the particular ABS image determined by using training data. Selecting threshold by means of threshold set has minimized summation of false rejection and false acceptance from training data. Threshold selected with the proposed method of this sample set are 435 and -1,000 for image data without and with contrast enhancement. The selected thresholds from Figures 5.6 and 5.8 are able to cluster Euclidean distance between the featured vectors obtained from the median of particular ABS. The ABS image needs to be classified as defected and non-defected shown in Figures 5.7 and 5.9, respectively. Images those possessed contrast enhancements are able to distinguish the defect and non-defect much more clearly. Table 5.1 shows summary of Type I and II error of clustering defected and non-defected ABS as false rejection and false acceptance, respectively. The error type I with image enhancement is decreased from 2.50 % without image enhancement to zero % and the error type II is decreased from 22.50 % without image enhancement to 2.50 %.

When analyzing the ROI for the occurrence of type II error, the result indicated that the position of defect is laid on the edge of ROI and has very small size. The histogram for the figure after contrast enhancement process cannot reveal any significance difference comparing to the non-defect ROI as show in Figure 5.10. Hence, the finding yields a false acceptance error. Nevertheless, this issue can be solved by optimizing the ROI size to enhance analysis sufficiently.

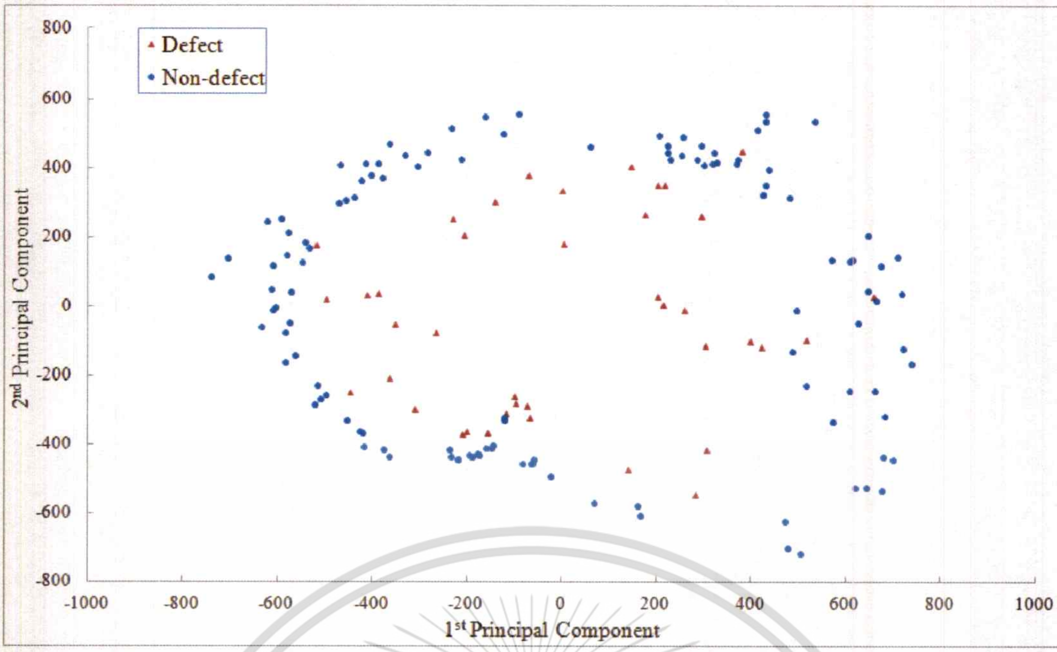

Figure 5.4: Two Principal Component without contrast enhancement

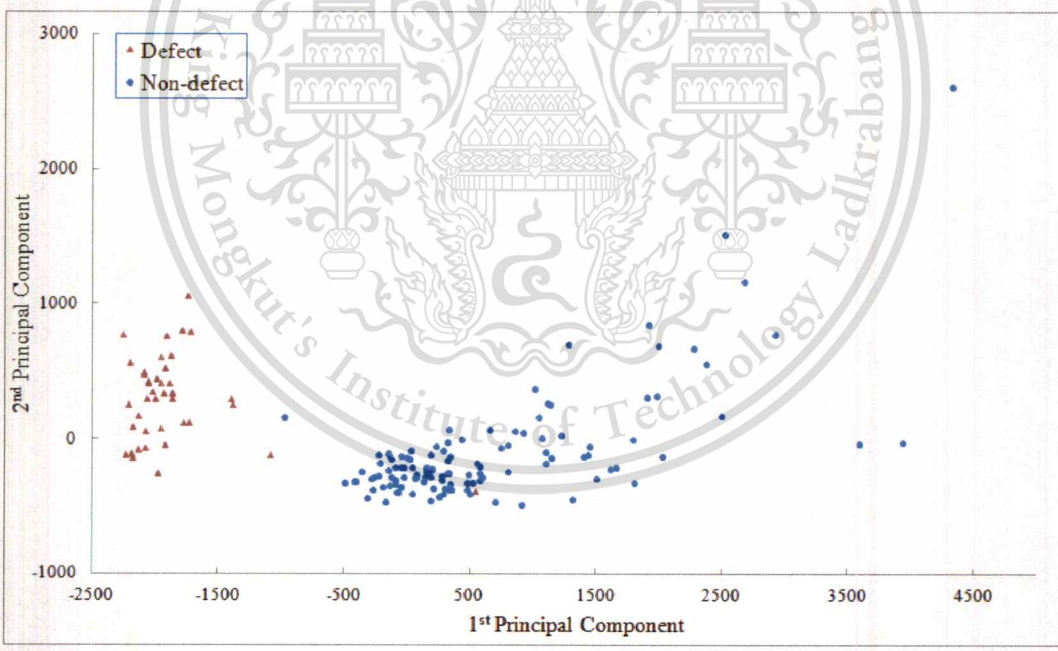

Figure 5.5: Two Principal Component with contrast enhancement

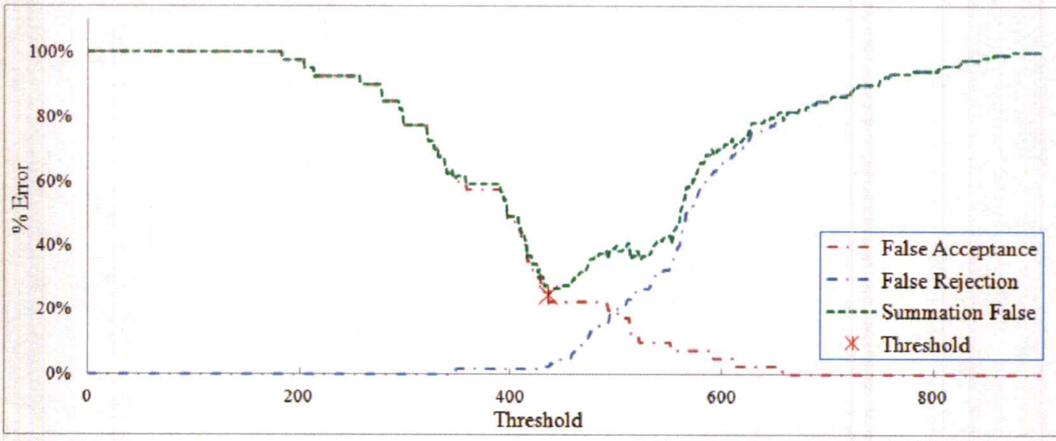

Figure 5.6: Threshold selection from Principal Component without contrast enhancement

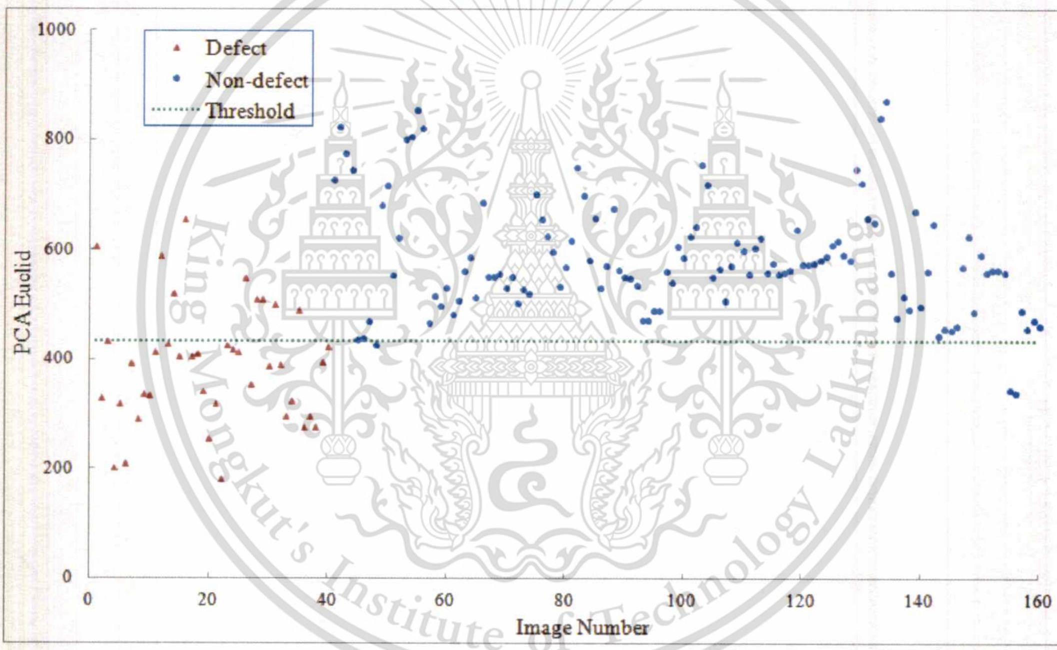

Figure 5.7: Euclidean distance and selected threshold without contrast enhancement

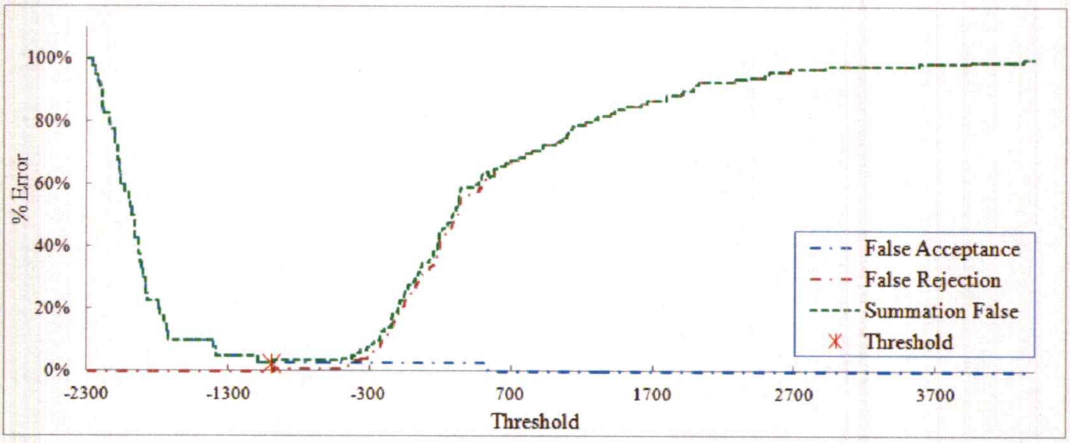

Figure 5.8: Threshold selection from Principal Component with contrast enhancement

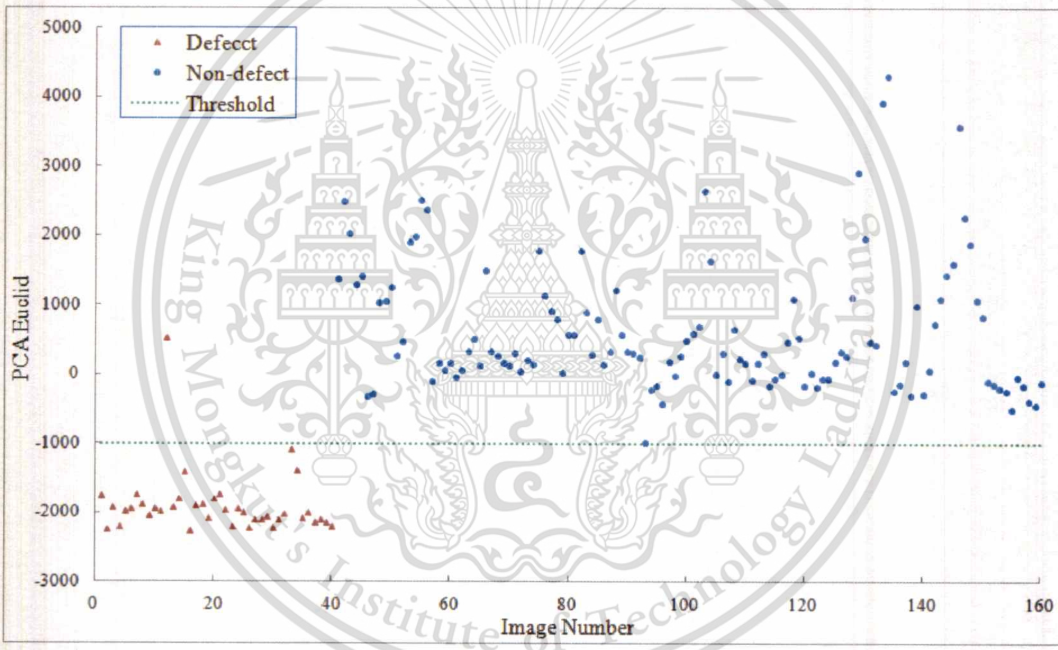

Figure 5.9: Euclidean distance and selected threshold with contrast enhancement

Table 5.1: Error type 1 and type 2

Error Type	Sample size	Quantity	% Error
Type I without contrast enhancement	120	3	2.5
Type II without contrast enhancement	40	9	22.5
Type I with contrast enhancement	120	0	0.0
Type II with contrast enhancement	40	1	2.5

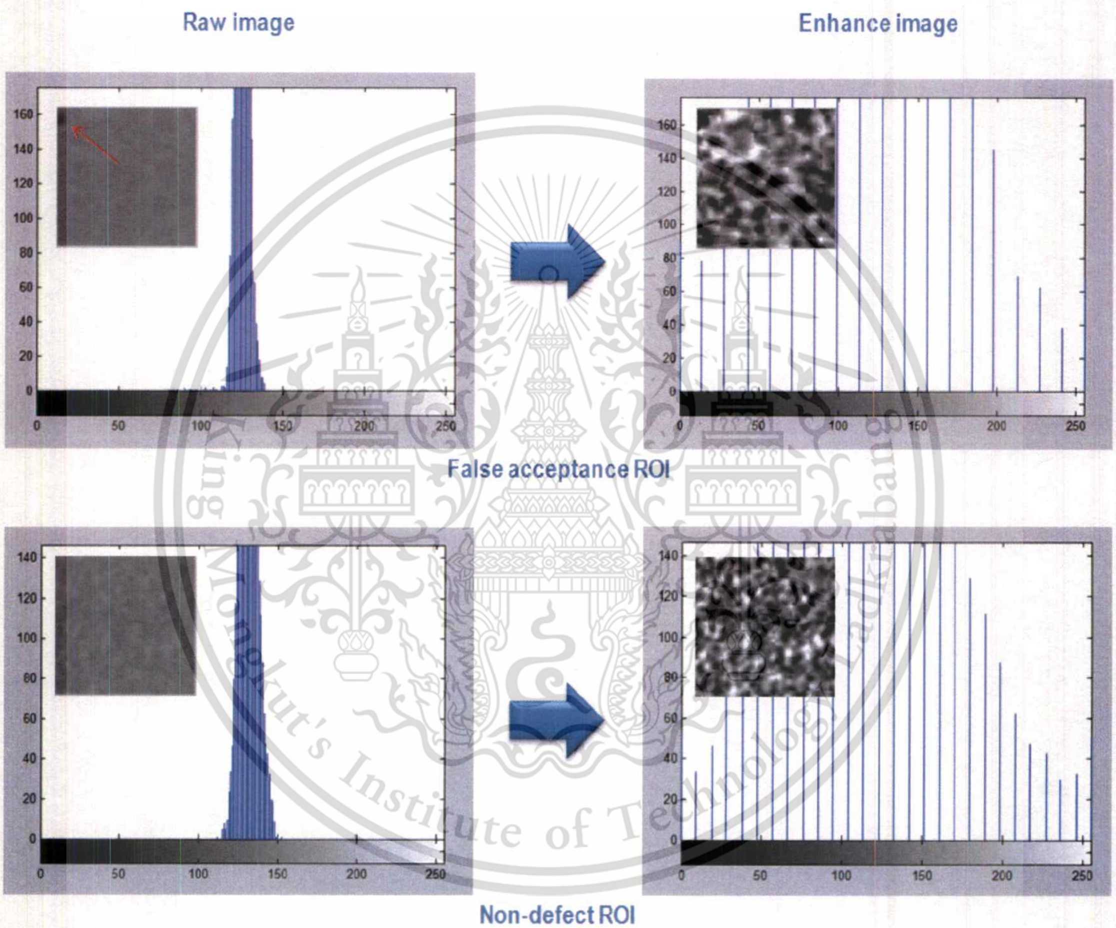

Figure 5.10: Histograms of false acceptance and non-defect

CHAPTER 6

CONCLUSION

The examination of contamination on the ABS should inspect on the proper microscope. The more appropriate microscope will be, the more visible and clearer defection will have. The defection cannot be detected if researcher had chosen an unsuitable microscope. Reason on how this research emphasized on the microscope is because the size of contamination aiming to examine 5 μm the particle sizes. This task requires the scope resolution at least 240,000 pixels. In this research, 1.3 Megapixel microscopes were used; resulting on more expediently detection of the contamination. However, with the consideration of processing time of image capturing, there should be an adjusting on the microscope to maintain least time but the effectiveness still remains as it was.

To solve the mentioned problem, Contrast enhancement techniques provide a multitude of choices for improving the visual quality of images. Because principle objective of this process is to find more suitable and accurate results than original image.

To obtain better results, the PCA method is used for visualization of complex data. Two PCs are sufficient for detecting the defect of the samples which could be use for demonstration of effective results.

The findings reveal that there still remains error type II which is the false acceptance. The methods from this research implies that the false acceptance cannot be eradicated. The false acceptance can affect to that the defected subjects are released to customer. The optimizing of ROI size to a proper level can enhance the proficiency of analysis capability. Furthermore for the future research, there should be the study of other methods collaterally for elimination of false acceptance.

REFERENCES

[1] Bo, Liu and et.al., "Contamination build-up on ABS and its effects on read/write performance of near-contact recording systems ", IEEE Journals & Magazines, vol.32, Sep. 1996, pp. 3884 - 3886.

[2] Zhang, S. and et.al., "Numerical and Experimental Study of the Particle Contamination in a Head/Media Interface", IEEE Transactions on Magnetics, vol.35, Sep. 1999, pp. 2442 - 2444.

[3] He, D.C. and Wang, L., "Texture unit, texture spectrum, and texture analysis", IEEE Transactions on Geoscience and Remote Sensing, vol.28, No.4, Jul. 1990, pp. 509 - 512.

[4] Karkanis, S.A. and et.al., "Classification of endoscopic images based on texture spectrum", Proceeding of Workshop on Machine Learning in Medical Aplications (ACAI'99), Jul. 1999, pp. 63 - 69.

[5] Novak, I. and Hocenski, Z., "Texture feature extraction for a visual inspection of ceramic tiles", ISIE Industrial Electronics, vol.3, Jun. 2005, pp. 1279 - 1283.

[6] Tomczak, L. and Mosorov, V., "Singular value decomposition for texture defect detection in visual inspection systems", MEMSTECH MEMS Design, May. 2006, pp. 131 - 133.

[7] Tomczak, L. and et.al., "Image Defect Detection Methods for Visual Inspection Systems", CADSM, 9th, CAD Systems in Microelectronics, Feb. 2007, pp. 454 - 456.

[8] Ertürk, S., "Digital Image Processing", 2003, Retrieved May 2013 from http://ik.itba.edu.ar/~jacoby/Image%20Processing/Books/Text%20Books/Digital %20Image%20Processing%20-%20Sarp%20Erturk.pdf.

[9] Kumar, M., "Satellite Remote Sensing and GIS Applications in Agricultural Meteorology", 2003, Retrieved May. 2013 from http://www.wamis.org/agm/ pubs/agm8/Paper-5.pdf.

[10] Fiete, R., "Modeling the Imaging Chain of Digital Cameras", 2010, Retrieved May 2013 from http://spie.org/samples/TT92.pdf.

[11] Wooten, A., "Integrating visual inspection capabilities into an automatic test equipment software environment", Proceedings of IEEE Autotestcon, Sep. 2006, pp. 486 - 495.

[12] Castleman, K. R., "Digital Image Processing", Prentice Hall, 1996.

[13] Junker, B. and Shalizi, C., "Principal Components Analysis", 2010, Retrieved Apr. 2013 from http://www.stat.cmu.edu/~cshalizi/490/10/pca/pca-handout.pdf.

[14] Moler, C., "Numerical Computing with MATLAB", 2004, Retrieved Jun. 2013 from http://www.mathworks.com/moler/interp.pdf.

[15] Jolliffe, I.T., "Principal Component Analysis", 2002, Retrieved Apr. 2013 from http://f3.tiera.ru/2/M_Mathematics/MV_Probability/MVsa_Statistics%20and%20applications/Jolliffe%20I.%20Principal%20Component%20Analysis.

[16] Joy, K., "EIGENVALUES AND EIGENVECTORS", 2000, Retrieved Nov. 2013 from http://www.idav.ucdavis.edu/education/CAGDNotes/Eigenvalues.pdf.

[17] Smith, L., "A tutorial on Principal Components Analysis", 2002, Retrieved Apr. 2013 from http://www.cs.otago.ac.nz/cosc453/student_tutorials/principal_components.pdf.

[18] Kumar, V., Sood, S. and Mishra S., "Introducing Effects in an Image: A MATLAB Approach", 2008, Retrieved Jun 2013 from http://hal.archives-ouvertes.fr/docs/00/32/16/24/PDF/Introducing_Effects_in_an_Image_-_A_MATLAB_Approach.pdf.

APPENDIX A

PUBLICATION

This work has also been published and presented in the International Innovative Scientific & Research Organization (IISRO) topic of the International Conference on Computer Networks and Information Technology (ICCNIT- 2013) at IBIS hotel in Bangkok, Thailand during June 29-30, 2013.

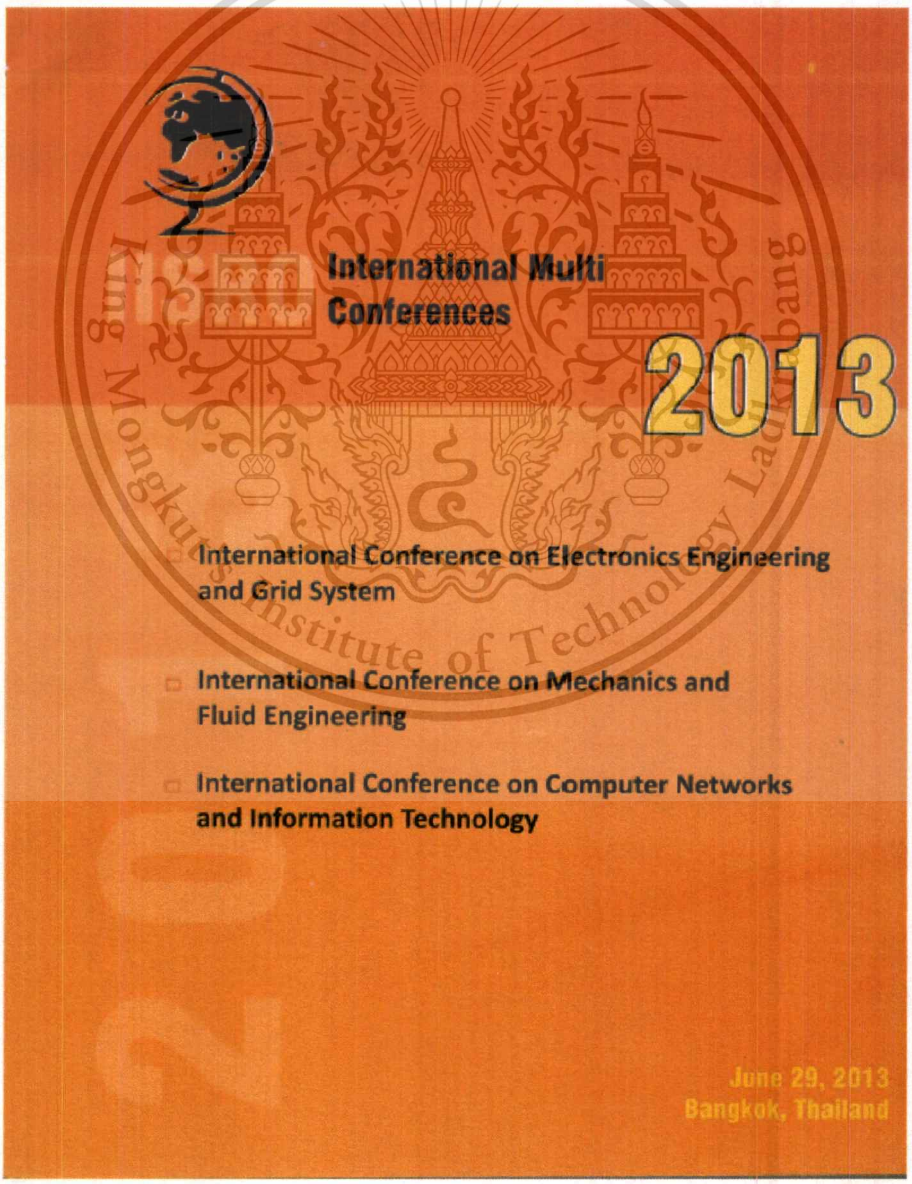

Contamination Detection on Air Bearing Surface

CHIEWCHAN TANGKONGKIET
College of Data Storage Innovation
King Mongkut's Institute of Technology Ladkrabang
Bangkok Thailand

PICHATE KUNAKORNVONG
College of Data Storage Innovation
King Mongkut's Institute of Technology Ladkrabang
Bangkok Thailand

PITIKHATE SOORAKSA
Faculty of Engineering
King Mongkut's Institute of Technology Ladkrabang
Bangkok Thailand

***Abstract*—Air Bearing Surface (ABS) is an important feature of a read and writes head in a Hard Disk Drive (HDD). Currently, contamination inspections are done using human operators and microscopes. The main problem of inspecting ABS with machine vision in the manufacturing process is contrast variation on the ABS. This research propose a new method for the reduction of contrast variation on ABS by using Contrast Enhancement, then extracts the feature of ABS using Principal Component Analysis (PCA), and then selecting the threshold for clustering defected and non-defected ABS by means of a threshold set which has a minimum summation of two types of error as false rejection and false acceptance from training data. The experimental results show that PCA with image enhancement can clearly separate defect and non-defect ABS. The result confirms its utility as an effective tool for machine vision.**

Keywords—Air Bearing Surface; Hard Disk Drive; Contrast; Contrast Enhancement; Principal Component Analysis component

I. INTRODUCTION

HDD manufacturing process has many influencing factors that will affect the performance of the HDD. Contamination is one of the key factors that might occur during Head Gimbal Assembly (HGA) process and could lead to lowered performance in the finished product. ABS is an important feature of the read and write head in the HDD that is used for precision head flight control. ABS controls the read and write head through the air pressure from the rotation of the disk. Thus, ABS is needed to be verify before the assembling process, any contamination on the ABS could reduce the HDD read and write performance. There is a study about the design, and the impact of contamination, including the characteristics which might be contaminated in the read and write head, ABS, and slider. The experimental results of investigations of contamination build-up on slider surfaces were reported by Bo Liu in 1996 [1]. In 2000, Shuyu Zhang provided a mathematical study and the impact of contamination of particles in the head and ABS [2].

Currently, no automatic machine could detect contamination on ABS. This research objective will aim to create algorithms that could detect contaminations on ABS using the machine vision system. The output from this machine could reduce the number of defects from the manufacturing process. Problems of visual inspection in the manufacturing process come from environmental factors, e.g. variation of lighting, which causes a different intensity of each image. For the examination with the vision system, there were some researchers who provided studies for manufacturing industries. In 1990, He and Wang described a new statistical approach to texture analysis, termed here the texture spectrum approach based on the proposed concept of texture unit [3]. Karkanis and team suggested a new approach to texture classification applied on lung endoscopic images by texture unit in 1999 [4]. In 2005, Novak and Hocenski had built a visual inspection system of ceramic tiles using the texture feature extraction methods based upon local binary patterns(LBP) [5]. An algorithm for texture defects detection was proposed by Tomczak and Mosorov in 2006. They used Singular Value Decomposition (SVD) and Fuzzy c-means clustering (FCM) to classify each region into two clusters [6]. The following year, they presented PCA and SVD methods to detect defect for automatic visual inspection systems [7].

This paper is organized as follows. Section II presents the image enhancement. Next, the feature extraction by PCA. Section III shows the experimental results. Finally, the conclusion will be drawn.

Figure 1. Three models of sample images.

II. METHOD

A. Contrast enhancement

The quality of an image perceived by a human could be improved by image enhancement techniques. Many standard ABS images when investigated on a color display were found to give insufficient information for image interpretation; on the other hand, by applying image enhancement techniques, these images will reveal more useful information. There is no conscious effort to improve the fidelity of the image with regards to some ideal form of the image. There exist a wide variety of techniques for improving image quality. Contrast is defined as the difference in grey level values in an image.

This paper is support by DSTAR, KMITL,NECTEC/ NSTDA and Seagate Technology (Thailand).

Also, as the ratio of the maximum to the minimum intensity over an image. Resolving power and detectability were strongly bearing by the Contrast Ratio. Images with a larger ratio were easier to interpret. Generally, current ABS images lack adequate contrast ratio and require contrast improvement.

Contrast enhancement techniques work by expanding the range of brightness values in an image. The aim is that the image will be displayed is a more effective manner as desire by the analyst. The density values in enhanced image literally pulled farther apart, that is, they expanded over a greater range. The increment of the visual contrast between two areas of the different was to established densities as the effect resulted. The main objective is to create greater discrimination between areas initially having a small difference in density values.

A high-contrast image spans the full range of gray-level values; therefore, a low-contrast image can be transformed into a high-contrast image by the method of remapping or stretching the gray-level values such that the final histogram spans the full range. The contrast stretch is often referred to as the dynamic range adjustment (DRA).

The simplest contrast stretch is a linear transformation that maps the lowest gray-level GL_{min} in the image to a new minimum GL'_{min} and the highest value GL_{max} in the image to a new maximum defined by GL'_{max} as shown in Fig. 2. This linear transformation is given by

$$f'(x,y) = INT\left\{\frac{GL'_{max} - GL'_{min}}{GL_{max} - GL_{min}}\left[f(x,y) - GL_{min}\right] + GL'_{min}\right\} \quad (1)$$

Where the INT function returns the integer value. If we wish to remap the image to the lowest gray-level GL_{min} in the image to zero and the highest value GL_{max} in the image to 255 (for an eight-bit image), with all other gray levels remapped linearly between zero and 255, to produce a high-contrast image that spans the full range of gray levels, the linear transform can be generalized to

$$f'(x,y) = INT\left\{\frac{255}{GL_{max} - GL_{min}}\left[f(x,y) - GL_{min}\right]\right\} \quad (2)$$

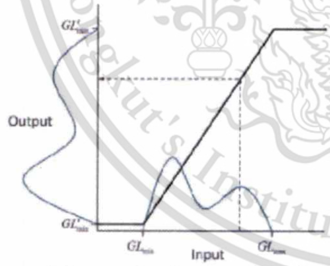

Figure 2. A Linear transform that remaps the gray levels.

The linear transformation for contrast enhancement spreads the gray-level values evenly over the full contrast range available. The relative shape of the histogram still remains unchanged but is widened to fill the range. The stretching of the histogram creates evenly distributed gaps between gray-level values in the image. Note that although the linear transformation will increase the contrast of the image, the steps between the populated gray-level values increase in contrast as well, which can result in visible contouring artifacts in the image.

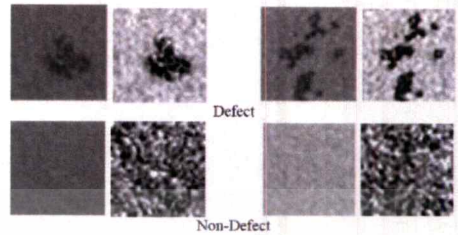

Figure 3. Contrast Enhancement Image

B. *Principal Component Analysis*

PCA, the generally referred to technique which used the sophisticated underlying mathematical principals in order to transform a number of possibly correlated variables into a smaller number of variables called principal components. Multispectral image data usually strongly correlated from one band to another. Particular picture element and its level on one band could extendible be predicted from the level of the same pixel in another band. PCS is a pre-processing transformation that creates new images from the uncorrelated values of different images. Accomplished by a linear transformation of variables that corresponds to a rotation and translation of the original coordinate system, PCA operates on all bands together and alleviates the difficulty of selecting appropriate bands associated with the band ratioing operation. The original band reflectance values less efficiently described the data than the principal component.

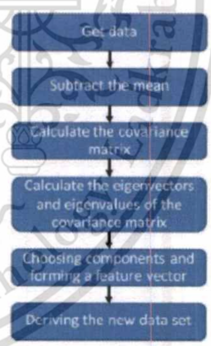

Figure 4. The PCA Method

Principal component transformation was used for spectral pattern recognition similar as well for the image enhancement. The least important principal components were dropped together when used before pattern recognition, permits to the omitted of the insignificant portion of data set and the avoidance of the additional computer time. The transformation functions are determined during the training stage. Principal component images could be analysed in various results, which are grayscale images, or any three component images that may be colour coded to form a colour composite. If little a priori information concerning the region is available, then the principal component enhancement techniques are particularly appropriate.

The first principal component is a single axis in space. When projecting each observation on that axis, the resulting values form a new variable and the variance of this variable is the maximum among all possible choices of the first axis. The second principal component is another axis in space, perpendicular to the first. Projecting the observations on this axis generates another new variable. The variance of this variable is the maximum among all possible choices of this second axis. The full set of principal components is as large as the original set of variables. However, it is commonplace for the sum of the variances of the first few principal components to exceed 80% of the total variance of the original data. The PCA method could be summarized as Fig. 4.

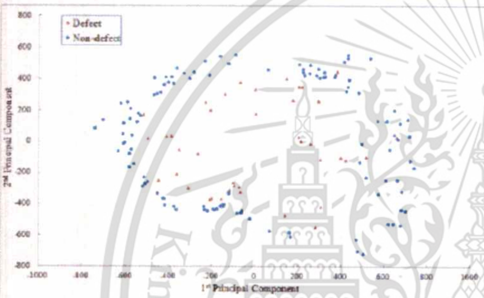

Figure 5. Two Principal Component without contrast enhancement

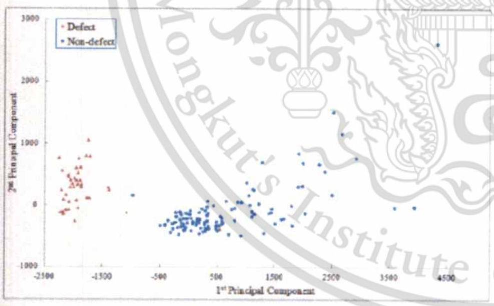

Figure 6. Two Principal Component with contrast enhancement

III. Experimental Results

In the experiments, ABS images were collected using a 1.3 megapixel camera. The database is a collection of 40 images from three ABS models as shown in Fig. 1. Four regions of Interest (ROI) from 40 ABS images were used. A total of 160 ROI samples are then available to test the new algorithm. The proposed method was implemented in MATLAB R2012a.

Using two PCA coefficients, it is possible to cluster defected and non-defected ABS. However, PCA coefficients alone without image enhancement were not good enough for clustering defected and non-defected ABS because the plot is sparse as shown in Fig. 5. Selected thresholds in Figs. 7 and 8 were calculated from the equation

$$\eta = \min(e_1 + e_2) \tag{3}$$

Where e_1 and e_2 are percentage of false rejection and false acceptance respectively. η is a preset threshold value for the particular ABS image determined by using training data. Selecting threshold by means of threshold set has minimum summation of false rejection and false acceptance from training data. Threshold selected with the proposed method of this sample set are 435 and -1,000, respectively. The selected thresholds from Figs. 7 and 8 are able to cluster Euclidean distance between the featured vectors obtained from the median of particular ABS. The ABS image needs to be classified as defected and non-defected shown in Figs. 9 and 10, respectively. Table 1 shows a summary of Type I and II error of clustering defected and non-defected ABS as false rejection and false acceptance respectively. The error type I with image enhancement is decreased from 2.50% without image enhancement to zero %, and the error type II is decreased from 22.50% without image enhancement to 2.50%.

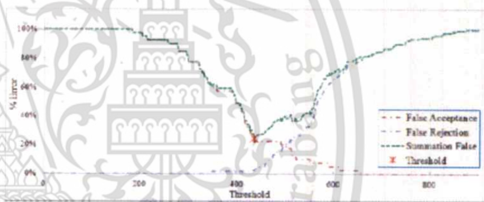

Figure 7. Threshold selection from Principal Component without contrast enhancement

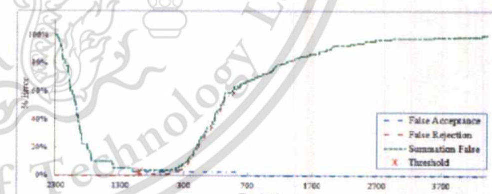

Figure 8. Threshold selection from Principal Component with contrast enhancement

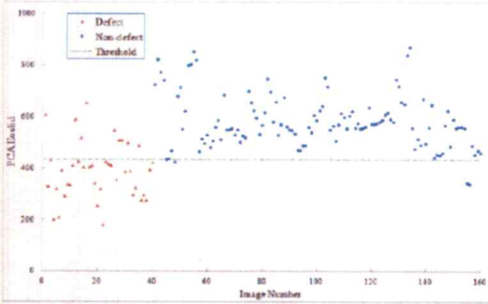

Figure 9. Euclidean distance and selected thrashold without contrast enhancement

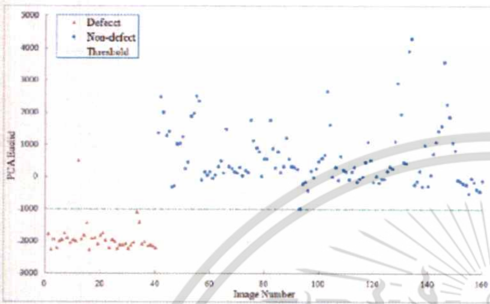

Figure 10. Euclidean distance and selected thrashold with contrast enhancement

TABLE I. ERROR TYPE I AND TYPE II

Error Type	Sample size	Quantity	%Error
Type I without image enhancement	120	3	2.50
Type II without image enhancement	40	9	22.50
Type I with image enhancement	120	0	0.00
Type II with image enhancement	40	1	2.50

IV. CONCLUSIONS

Image enhancement help decreases contrast variations. Its the principal objective is to process an image for better perception during the analyzing process. This provides more accurate results than using the original images alone. Image enhancement techniques provide an alternative for improving the visual quality of ABS images. Two PCA coefficients are sufficient for detecting the defect, that have been demonstrated with the collected ABS image database to provide a more effective and accurate result.

ACKNOWLEDGMENT

The authors would like to acknowledge The College of Data Storage Innovation King Mongkut's Institute of Technology Ladkrabang, NECTEC/NSTDA and also Seagate Technology (Thailand) for their equipment and financial supports.

REFERENCES

[1] Bo Liu, Hu, S.B., Soo K.T., Wang J.P., Ng S.H., Lee C.S., "Contamination build-up on ABS and its effects on read/write performance of near-contact recording systems ", IEEE Journals & Magazines, vol.32, Sep 1996, pp. 3884 - 3886.

[2] Shuyu, Z. et.al., "Numerical and Experimental Study of the Particle Contamination in a Head/Media Interface", IEEE Transactions on Magnetics, vol.35, Sep.1999, pp.2442-2444.

[3] He, D.C. and Wang, L. "Texture unit, texture spectrum, and texture analysis", IEEE Transactions on Geoscience and Remote Sensing, vol.28, No.4, Jul. 1990, pp.509-512.

[4] Karkanis, S.A. et.al., "Classification of endoscopic images based on texture spectrum", Proceeding of Workshop on Machine Learning in Medical Aplications (ACAI'99), Jul. 1999, pp.63-69

[5] Novak I., Hocenski Z., "Texture feature extraction for a visual inspection of ceramic tiles", ISIE Industrial Electronics, vol.3, June 2005, pp. 1279 – 1283.

[6] Tomczak L., Mosorov V., "Singular value decomposition for texture defect detection in visual inspection systems", MEMSTECH MEMS Design, May 2006, pp. 131 – 133.

[7] Tomczak L.,Mosorov V., Sankowski D., Nowakowski J., "Image Defect Detection Methods for Visual Inspection Systems", CADSM, 9th, CAD Systems in Microelectronics, Feb. 2007, pp. 454 - 456 .

APPENDIX B

Eigenvalue and Eigenvector

What are Eigenvalues and Eigenvectors?

Let A be an n × n matrix and consider the vector equation

$$A\vec{v} = \lambda\vec{v}$$

where λ is a scalar value.

It is clear that if $\vec{v} = \vec{0}$, we have a solution for any value of λ. A value of λ for which the equation has a solution with $\vec{v} \neq \vec{0}$ is called an eigenvalue or characteristic value of the matrix A. The corresponding solutions $\vec{v} \neq \vec{0}$ are called eigenvectors or characteristic vectors of A. In the problem above, we are looking for vectors that when multiplied by the matrix A, give a scalar multiple of itself.

The set of eigenvalues of A is commonly called the spectrum of A and the largest of the absolute values of the eigenvalues is called the spectral radius of A.

Eigenvalues are also called proper values ("eigen" is German for the word "own" or "proper"). Eigenvalues were initial used by Leonhard Euler in 1743 in connection with the solution to an n^{th} order linear differential equation with constant coefficients.

How Do We Calculate the Eigenvalues?

It is easy to see that the equation

$$A\vec{v} = \lambda\vec{v}$$

can be rewritten as

$$(A - \lambda I)\vec{v} = 0$$

where I is the identity matrix. A matrix equation of this form can only be solved if the determinant of the matrix is nonzero (see Cramer's Rule) – that is, if

$$\det(A-\lambda I)=0$$

Since this equation is a polynomial in , commonly called the characteristic polynomial, we only need to find the roots of this polynomial to find the eigenvalues.

We note that to get a complete set of eigenvalues, one may have to extend the scope of this discussion into the field of complex numbers.

How Do We Calculate the Eigenvectors?

The eigenvalues must be determined first. Once these are known, the corresponding eigenvectors can be calculated directly from the linear system

$$(A-\lambda I)\vec{v}=0$$

It should be noted that if $\vec{v}$ is an eigenvector, then so is $k\vec{v}$ for any scalar k.

Right Eigenvectors

Given an eigenvalue λ, The eigenvector $\vec{r}$ that satisfies

$$A\vec{r}=\lambda\vec{r}$$

is sometimes called a (right) eigenvector for the matrix A corresponding to the eigenvalue λ. If $\lambda_1,\lambda_2,\ldots,\lambda_r$ are the eigenvalues and $\vec{r}_1,\vec{r}_2,\ldots,\vec{r}_r$ are the corresponding right eigenvectors, then is easy to see that the set of right eigenvectors form a basis of a vector space. If this vector space is of dimension n, then we can construct an n × n matrix R whose columns are the components of the right eigenvectors, which has the property that

$$AR=R\Lambda$$

where Λ is the diagonal matrix

$$\Lambda = \begin{bmatrix} \lambda_1 & 0 & 0 & \cdots & 0 \\ 0 & \lambda_2 & 0 & \cdots & 0 \\ 0 & 0 & \lambda_3 & \cdots & 0 \\ \vdots & \vdots & \vdots & \ddots & \vdots \\ 0 & 0 & 0 & 0 & \lambda_n \end{bmatrix}$$

whose diagonal elements are the eigenvalues. By appropriate numbering of the eigenvalues and eigenvectors, it is possible to arrange the columns of the matrix R so that $\lambda_1 \geq \lambda_2 \geq \ldots \geq \lambda_n$.

Left Eigenvectors

A vector $\vec{l}$ so that

$$\vec{l}^{\,T} A = \lambda \vec{l}^{\,T}$$

is called a left eigenvector for A corresponding to the eigenvalue λ. If $\lambda_1, \lambda_2, \ldots, \lambda_r$ are the eigenvalues and $\vec{l}_1, \vec{l}_2, \ldots, \vec{l}_r$ are the corresponding left eigenvectors, then is easy to see that the set of left eigenvectors form a basis of a vector space. If this vector space is of dimension n, then we can construct an n × n matrix L whose rows are the components of the left eigenvectors, which has the property that

$$LA = \Lambda L$$

It is possible to choose the left eigenvectors $\vec{l}_1, \vec{l}_2, \ldots$ and right eigenvectors $\vec{r}_1, \vec{r}_2, \ldots$ so that

$$\vec{l}_i \cdot \vec{r}_j = \begin{cases} \begin{cases} 1 & if \quad i = j \\ 0 & otherwise \end{cases} \end{cases}$$

This is easily done if we define $L = R^{-1}$ and define the components of the left eigenvectors to be the elements of the respective rows of L. Beginning with $AR = R\Lambda$ and multiplying both sides on the left by R^{-1}, we obtain

$$R^{-1} AR = \Lambda$$

and multiplying on the right by R^{-1}, we have

$$R^{-1}A = \Lambda R^{-1}$$

which implies that any row of R^{-1} satisfies the properties of a left eigenvector.

Diagonalization of a Matrix

Given an n × n matrix A, we say that A is diagonalizable if there is a matrix X so that

$$X^{-1}AX = \Lambda$$

where

$$\Lambda = \begin{bmatrix} \lambda_1 & 0 & 0 & \cdots & 0 \\ 0 & \lambda_2 & 0 & \cdots & 0 \\ 0 & 0 & \lambda_3 & \cdots & 0 \\ \vdots & \vdots & \vdots & \ddots & \vdots \\ 0 & 0 & 0 & 0 & \lambda_n \end{bmatrix}$$

It is clear from the above discussions that if all the eigenvalues are real and district, then we can use the matrix of right eigenvectors R as X.

EXAMPLE: Find the eigenvalues and eigenvectors of the matrix

$$A = \begin{pmatrix} 1 & -3 & 3 \\ 3 & -5 & 3 \\ 6 & -6 & 4 \end{pmatrix}$$

SOLUTION:

FINDING EIGENVALUES

To do this, we find the values of λ which satisfy the characteristic equation of the matrix A, namely those values of λ for which

$$\det\left(A - \lambda I\right) = 0,$$

where I is the 3x3 identity matrix.

Form the matrix $A-\lambda I$:

$$A-\lambda I=\begin{pmatrix}1 & -3 & 3\\ 3 & -5 & 3\\ 6 & -6 & 4\end{pmatrix}-\begin{pmatrix}\lambda & 0 & 0\\ 0 & \lambda & 0\\ 0 & 0 & \lambda\end{pmatrix}=\begin{pmatrix}1-\lambda & -3 & 3\\ 3 & -5-\lambda & 3\\ 6 & -6 & 4-\lambda\end{pmatrix}$$

Notice that this matrix is just equal to A with λ subtracted from each entry on the main diagonal.

Calculate $\det(A-\lambda I)$:

$$\begin{aligned}\det(A-\lambda I) &=(1-\lambda)\begin{vmatrix}-5-\lambda & 3\\ -6 & 4-\lambda\end{vmatrix}-(-3)\begin{vmatrix}3 & 3\\ 6 & 4-\lambda\end{vmatrix}+3\begin{vmatrix}3 & -5-\lambda\\ 6 & -6\end{vmatrix}\\ &=(1-\lambda)\left((-5-\lambda)(4-\lambda)-(3)(-6)\right)+3\left(3(4-\lambda)-3\times 6\right)+3\left(3\times(-6)-(-5-\lambda)6\right)\\ &=(1-\lambda)\left(-20+5\lambda-4\lambda+\lambda^2+18\right)+3(12-3\lambda-18)+3(-18+30+6\lambda)\\ &=(1-\lambda)\left(-2+\lambda+\lambda^2\right)+3(-6-3\lambda)+3(12+6\lambda)\\ &=-2+\lambda+\lambda^2+2\lambda-\lambda^2-\lambda^3-18-9\lambda+36+18\lambda\\ &=16+12\lambda-\lambda^3.\end{aligned}$$

Therefore

$$\det(A-\lambda I)=-\lambda^3+12\lambda+16$$

REQUIRED: To find solutions to $\det(A-\lambda I)=0$ i.e., to solve

$$\lambda^3-12\lambda-16=0$$

Look for integer valued solutions. Such solutions divide the constant term (-16). The list of possible integer solutions is $\pm1,\pm2,\pm4,\pm8,\pm16$.

Taking $\lambda=4$, we find that

$$4^3-12.4-16=0.$$

Now factor out $\lambda-4$:

$$(\lambda-4)\left(\lambda^2+4\lambda+4\right)=\lambda^3-12\lambda^2+16.$$

Solving $\lambda^2+4\lambda+4$ by formula gives

$$\lambda=\frac{-4\pm\sqrt{4^2-4\cdot1\cdot4}}{2}=\frac{-4\pm0}{2},$$

and so $\lambda=-2$ (a repeated root).

Therefore, the eigenvalues of A are $\lambda=4,-2$. ($\lambda=-2$ is a repeated root of the characteristic equation.)

FINDING EIGENVECTORS

Once the eigenvalues of a matrix (A) have been found, we can find the eigenvectors by Gaussian Elimination.

STEP 1: For each eigenvalue λ, we have

$$(A-\lambda I)x=0,$$

where x is the eigenvector associated with eigenvalue λ.

STEP 2: Find x by Gaussian elimination. That is, convert the augmented matrix

$$(A-\lambda I\vdots 0)$$

to row echelon form, and solve the resulting linear system by back substitution.

We find the eigenvectors associated with each of the eigenvalues

Case 1: $\lambda=4$

We must find vectors x which satisfy $(A-\lambda I)x=0$.

First, form the matrix $A-4I$:

$$A-4I=\begin{pmatrix}-3 & -3 & 3\\ 3 & -9 & 3\\ 6 & -6 & 0\end{pmatrix},$$

Construct the augmented matrix $(A-\lambda I \vdots 0)$ and convert it to row echelon form

$$\begin{pmatrix} -3 & -3 & 3 & 0 \\ 3 & -9 & 3 & 0 \\ 6 & -6 & 0 & 0 \end{pmatrix}\begin{matrix} R1 \\ R2 \\ R3 \end{matrix} \quad R1 \to \underline{-1/3} \times R3 \quad \begin{pmatrix} 1 & 1 & -1 & 0 \\ 3 & -9 & 3 & 0 \\ 6 & -6 & 0 & 0 \end{pmatrix}\begin{matrix} R1 \\ R2 \\ R3 \end{matrix}$$

$$\begin{matrix} R2 \to R2 - 3 \times R1 \\ R3 \to \underline{R3 - 6} \times R1 \end{matrix} \quad \begin{pmatrix} 1 & 1 & -1 & 0 \\ 0 & -12 & 6 & 0 \\ 0 & -12 & 6 & 0 \end{pmatrix}\begin{matrix} R1 \\ R2 \\ R3 \end{matrix}$$

$$R2 \to \underline{-1/12} \times R2 \quad \begin{pmatrix} 1 & 1 & -1 & 0 \\ 0 & 1 & -1/2 & 0 \\ 0 & -12 & 6 & 0 \end{pmatrix}\begin{matrix} R1 \\ R2 \\ R3 \end{matrix}$$

$$R3 \to \underline{R3 + 12} \times R2 \quad \begin{pmatrix} 1 & 1 & -1 & 0 \\ 0 & 1 & -1/2 & 0 \\ 0 & 0 & 0 & 0 \end{pmatrix}\begin{matrix} R1 \\ R2 \\ R3 \end{matrix}$$

$$R1 \to \underline{R1} - R2 \quad \begin{pmatrix} 1 & 0 & -1/2 & 0 \\ 0 & 1 & -1/2 & 0 \\ 0 & 0 & 0 & 0 \end{pmatrix}\begin{matrix} R1 \\ R2 \\ R3 \end{matrix}$$

Rewriting this augmented matrix as a linear system gives

$$\begin{aligned} x_1 - 1/2x_3 &= 0 \\ x_2 - 1/2x_3 &= 0 \end{aligned}$$

So the eigenvector x is given by:

$$x = \begin{pmatrix} x_1 = \dfrac{x_3}{2} \\ x_2 = \dfrac{x_3}{2} \\ x_3 \end{pmatrix} = x_3 \begin{pmatrix} \dfrac{1}{2} \\ \dfrac{1}{2} \\ 1 \end{pmatrix}$$

For any real number $x_3 \neq 0$. Those are the eigenvectors of A associated with the eigenvalue $\lambda = 4$.

Case 2: $\lambda = -2$

We seek vectors x for which $(A - \lambda I)x = 0$.

Form the matrix $A - (-2)I = A + 2I$

$$A + 2I = \begin{pmatrix} 3 & -3 & 3 \\ 3 & -3 & 3 \\ 6 & -6 & 6 \end{pmatrix}$$

Now we construct the augmented matrix $(A - \lambda I \vdots 0)$ and convert it to row echelon form

$$\begin{array}{c} \begin{pmatrix} 3 & -3 & 3 & 0 \\ 3 & -3 & 3 & 0 \\ 6 & -6 & 6 & 0 \end{pmatrix} \begin{array}{l} R1 \\ R2 \\ R3 \end{array} \end{array} \quad R1 \to \underline{1/3} \times R3 \quad \begin{pmatrix} 1 & -1 & 1 & 0 \\ 3 & -3 & 3 & 0 \\ 6 & -6 & 6 & 0 \end{pmatrix} \begin{array}{l} R1 \\ R2 \\ R3 \end{array}$$

$$\begin{array}{l} R2 \to R2 - 3 \times R1 \\ R3 \to \underline{R3 - 6} \times R1 \end{array} \begin{pmatrix} 1 & 1 & -1 & 0 \\ 0 & 0 & 0 & 0 \\ 0 & 0 & 0 & 0 \end{pmatrix} \begin{array}{l} R1 \\ R2 \\ R3 \end{array}$$

When this augmented matrix is rewritten as a linear system, we obtain

$$x_1 + x_2 - x_3 = 0,$$

so the eigenvectors x associated with the eigenvalue $\lambda = -2$ are given by:

$$x = \begin{pmatrix} x_1 = x_3 - x_2 \\ x_2 \\ x_3 \end{pmatrix}$$

Thus

$$x = \begin{pmatrix} x_3 - x_2 \\ x_2 \\ x_3 \end{pmatrix} = x_3 \begin{pmatrix} 1 \\ 0 \\ 1 \end{pmatrix} + x_2 \begin{pmatrix} -1 \\ 1 \\ 0 \end{pmatrix} \text{ for any } x_2, x_3 \in \mathbb{R} \setminus \{0\}$$

are the eigenvectors of A associated with the eigenvalue $\lambda = -2$.

AUTHOR BIOGRAPHY

Name-Surname: Mr. Chiewchan Tangkongkiet

Date of Birth: June 12nd, 1986

Present Address: 5/56, Moo 2, Supalai ville, Soi Bearing 58, Sukhumvit 107 Rd., Tambol Samrongnua, Amphur Muang, Samutprakarn, Thailand 10270

Education: 2005-2008: Bachelor degree in Electrical-Mechanical Manufacturing Engineering, Kasetsart university.

Scholarships: 2011-2012 Scholarship for study in Master of Engineering in Data Storage Technology (English program) by NSTDA, KMITL and Seagate Technology (Thailand) Ltd.

Publications: Tangkongkiet C., "CONTAMINATION DETECTION ON AIR BEARING SURFACE", ICCNIT 2013,0 International Conference on Computer Network and Information Technology at Bangkok, Thailand, June 29-30, 2013.

Experience:

2008-Present Seagate Technology (Thailand) Ltd.

- Mechanical Design Engineer of Advanced Manufacturing Engineering